Grant Agreement No.: 226479

SafeLand

Living with landslide risk in Europe: Assessment,
effects of global change, and risk management strategies

7th Framework Programme
Cooperation Theme 6 Environment (including climate change)
Sub-Activity 6.1.3 Natural Hazards

Deliverable D2.7

Case studies of environmental and societal impact of landslides –
<u>Part A:</u> Case studies for environmental (physical) vulnerability

Work Package WP2.2 – Vulnerability to landslides

Deliverable/Work Package Leader: AUTh   Revision: 1 – Final

April, 2011

Rev.	Deliverable Responsible	Controlled by	Date
0	AUTh-ICG	ICG	21-03-2011
1	AUTh-ICG	ICG	28-03-2011
2			

Deliverable D2.7   Rev. No: 1
Case studies of environmental and societal impact of landslides –
 Part A: Case studies for environmental (physical) vulnerability   Date: 2010-04-01

SUMMARY

The present report comprises the first Part (Part A) of Deliverable D2.7 "Case studies of environmental and societal impact of landslides" that is aimed at providing representative case studies for environmental (physical) vulnerability, based on the methodologies proposed in Safeland deliverable D2.5: "Physical vulnerability of elements at risk to landslides: Methodology for evaluation, fragility curves and damage states for buildings and lifelines", Pitilakis et al. (2010). The applications of the methods for assessing physical vulnerability concern different affected facilities including single buildings or building aggregates and lifelines, different landslide hazards and triggering mechanisms (intense precipitation, earthquake) and various analysis scales (small, medium, site specific).

Note about contributors

The following organisations contributed to the work described in this deliverable:

Lead partner responsible for the deliverable:
[AUTH]
Deliverable prepared by:
Kyriazis Pitilakis, Stavroula Fotopoulou, Sotiris Argyroudis, Dimitris Pitilakis, Kwstas Senetakis, Kostantinos Treulopoulos, Evi Riga

Partner responsible for quality control:
[ICG]
Deliverable reviewed by:
Bjørn Vidar Vangelsten

Other contributors:
[UNISA] : Leonardo Cascini, Settimio Ferlisi, Giovanni Pisciotta

Deliverable D2.7
Case studies of environmental and societal impact of landslides –
 Part A: Case studies for environmental (physical) vulnerability

Rev. No: 1

Date: 2011-04-01

CONTENTS

Deliverable D2.7   Rev. No: 1
Case studies of environmental and societal impact of landslides –
 Part A: Case studies for environmental (physical) vulnerability   Date: 2011-04-01

1   INTRODUCTION

This report presents representative applications of the methods for assessing physical vulnerability of buildings and roads affected by different landslide hazards and at different scales. The methods are described in Safeland deliverable D2.5: "Physical vulnerability of elements at risk to landslides: Methodology for evaluation, fragility curves and damage states for buildings and lifelines", Pitilakis et al. (2010).

In particular, the physical vulnerability in terms of building's (homogeneous) aggregates due to different slow moving landslide hazards is assessed at the territory of the National Basin Authority of "Liri-Garigliano" and "Volturno" rivers, Central-Southern Italy by UNISA at small scale (1:100.000). Moreover, they estimated the vulnerability of smaller building aggregated levels affected by slow movements at two study areas (scale 1:25.000) within the already investigated territory. In addition, they contributed to the quantification of the vulnerability of buidings subjected to rainfall induced slow moving landslides located at the test site of San Pietro in Guarano, Cosenza Province, southern Italy (scale 1:2000).

The physical vulnerability of a representative RC building subjected to earthquake triggered slow moving landslide hazards located near the Kato Achaia (western Greece) slope's crest is investigated by AUTH. Finally, the vulnerability of the roadway system of Grevena in Greece due to earthquake triggered landslides is assessed (AUTH). The method has been proposed for seismically induced displacements but it could be equally implemented for the case of hydrological hazards (intense precipitation).

Deliverable D2.7   Rev. No: 1
Case studies of environmental and societal impact of landslides –
 Part A: Case studies for environmental (physical) vulnerability   Date: 2011-04-01

2   APPLICATION TO BUILDING AGGREGATES AT THE TERRITORY OF THE NATIONAL BASIN AUTHORITY OF "LIRI-GARIGLIANO" AND "VOLTURNO" RIVERS, CENTRAL-SOUTHERN ITALY (SCALE: 1:100.000) (UNISA)

The physical vulnerability of buildings aggregates at the territory of the National Basin Authority of "Liri-Garigliano" and "Volturno" rivers, Central-Southern Italy (scale: 1:100.000) is assessed. The method is briefly described in Subsection 6.1.

2.1   REVIEW OF THE METHOD

The framework of the procedure, described in the SafeLand deliverable D2.5, Pitilakis et al. (2010) for the estimation of the physical vulnerability to slow-moving landslides at small scale is shown in Figure 2.1.1. According to the "consequence model" described by Wong et al. (1997), this framework was established considering that the expected damage to building aggregates can be related to several factors, often concomitant; among these, the spatial distribution of the phenomena and the density of built-up areas within a given territory.
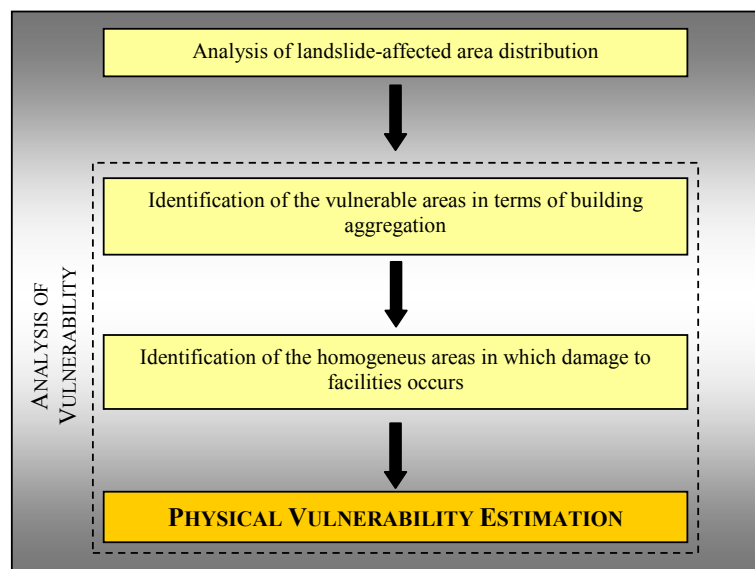

Figure 2.1.1 General framework for the estimation of the physical vulnerability to slow-moving landslides at small scale (modified from Pisciotta 2008).

2.2   APPLICATION

The procedure based on the framework of Figure 2.1.1 was tested in large study areas of the territory of the National Basin Authority of "Liri-Garigliano and Volturno" (NBA-LGV) rivers extending for about 12,000 km^2 in central-southern Italy (Fig. 2.2.1). This territory is composed of two main sub-territories corresponding to the Liri-Garigliano and the Volturno river basins and it involves – partially or totally – the territories of 5 Regions (Abruzzo, Campania, Lazio, Molise and Puglia), 11 Provinces and 450 Municipalities (Fig. 2.2.1).

Deliverable D2.7
Case studies of environmental and societal impact of landslides –
 Part A: Case studies for environmental (physical) vulnerability
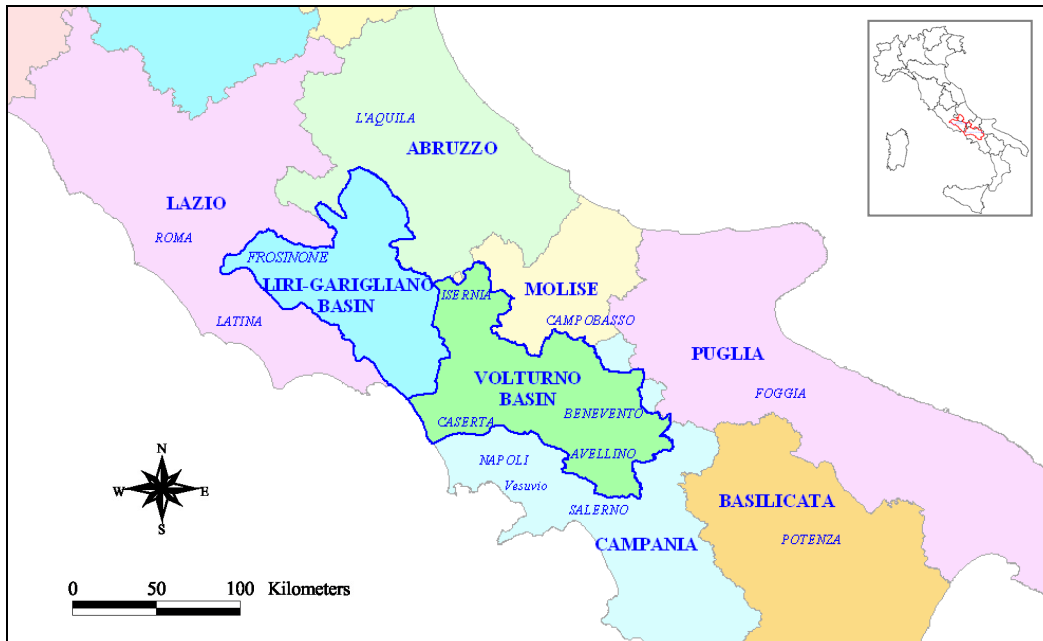
Rev. No: 1

Date: 2011-04-01

Figure 2.2.1 The territory of the National Basin Authority of Liri-Garigliano and Volturno rivers.
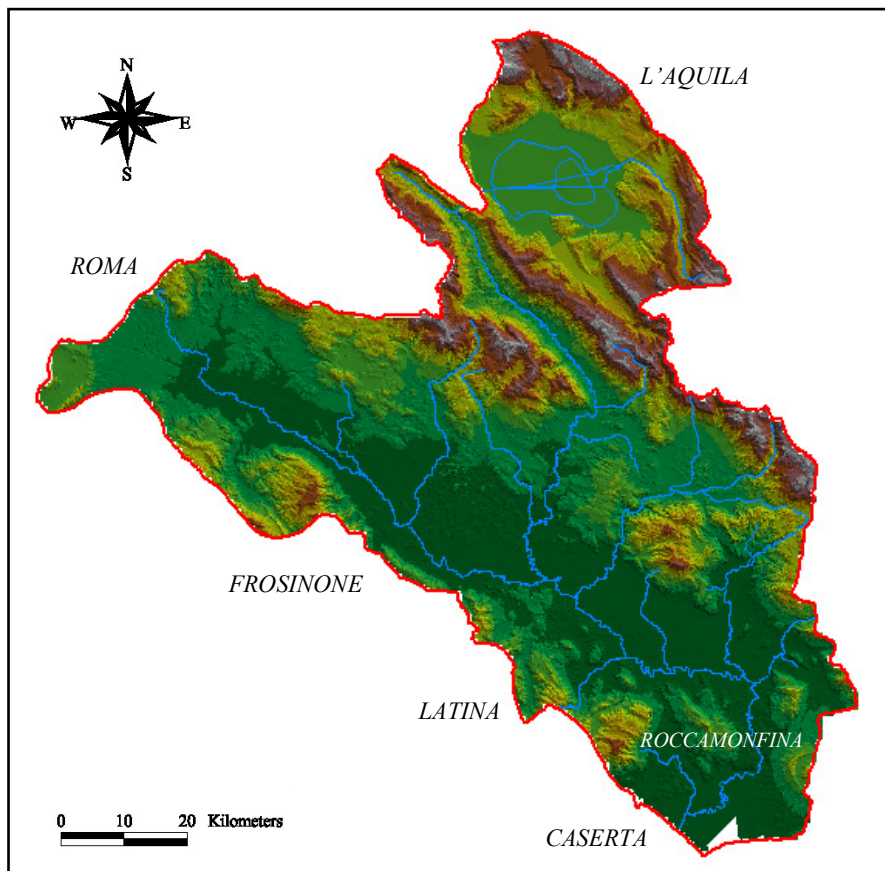
Figure 2.2.2 Digital Elevation Model of the Liri-Garigliano basin.

Deliverable D2.7   Rev. No: 1
Case studies of environmental and societal impact of landslides –
 Part A: Case studies for environmental (physical) vulnerability   Date: 2011-04-01

The Liri river rises near the Municipality of Cappadocia, at an elevation of about 995 m a.s.l. and joins with the Garigliano river at about 60 m a.s.l.; then, the two rivers flow together into the Tyrrhenian Sea. The Liri-Garigliano basin, covering a surface of about 5,124 km^2 (Fig. 2.2.2) has proper geomorphological features, namely: flat zones in the coastal areas, at the mouth of the river and in the deep valleys; hilly zones in the centre and north-west presenting Mesozoic and Pliocene deposits with a prevailing clay matrix and Quaternary Age deposits; and mountainous zones in the northern, north-eastern and eastern parts, where Mesozoic and Cainozoic carbonate complexes prevail (Cascini, 2003).

The Volturno, 175 km long, is the most important river in southern Italy, with a basin covering about 5,640 km^2. It is composed of two main sub-basins associated with the Volturno itself and the Calore river (132 km long) (Fig. 2.2.3).

The central-western zone of the Volturno river basin is characterized by the presence of Mesozoic and Cainozoic carbonatic reliefs. The eastern area mainly consists of hills presenting Mesozoic and Cainozoic terrigenous, calcareous, arenaceous and pelitic deposits. In the western zone there are pyroclastic deposits that originated from the activity of the Roccamonfina, Campi Flegrei and Somma-Vesuvius volcano complexes (Cascini, 2003).
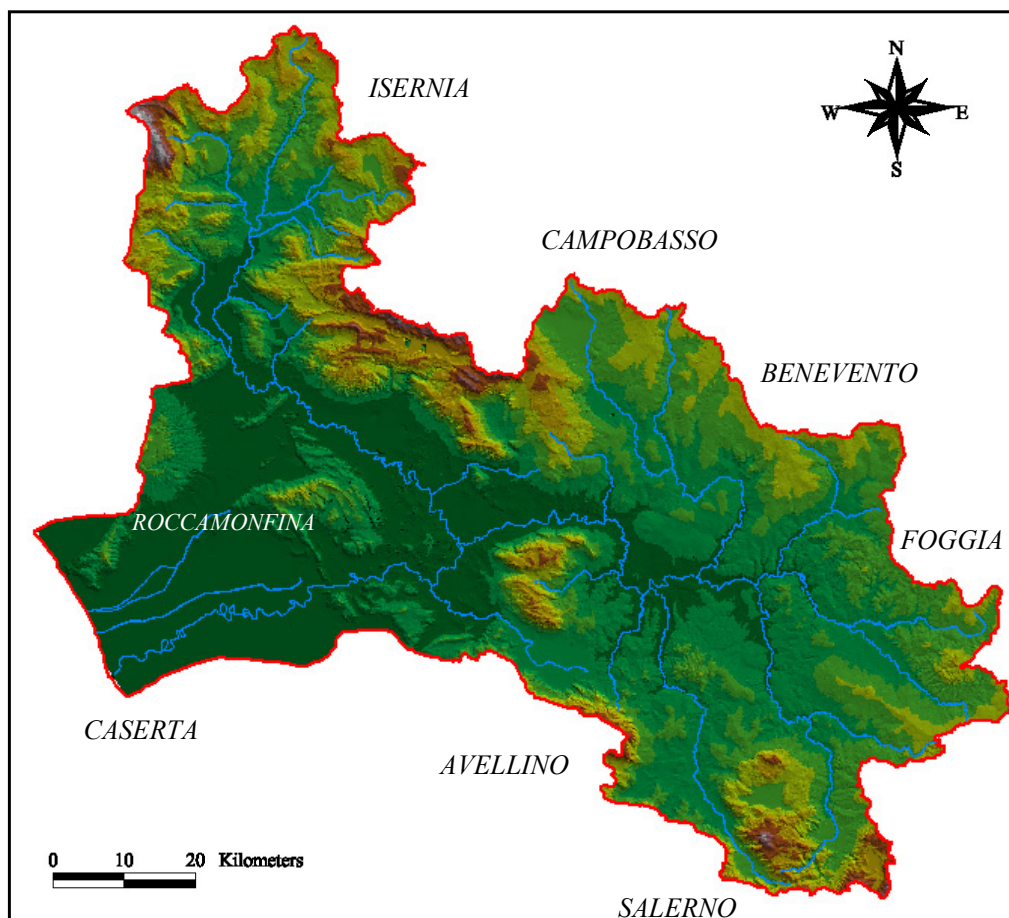

Figure 2.2.3 Digital Elevation Model of the Volturno basin.

Deliverable D2.7
Case studies of environmental and societal impact of landslides –
 Part A: Case studies for environmental (physical) vulnerability

Rev. No: 1

Date: 2011-04-01

Slow-moving landslides – namely, rotational slides, earth flows, rotational slides-earth flows, earth flows-creeps, creeps and deep-seated gravitational movements – affect 10% of the whole NBA-LGV territory and they are widespread especially in the Volturno basin. Moreover, 73% of the total number ($\approx$ 18,000) of landslides inventoried in a very accurate map at 1:25,000 scale are located in the Volturno basin, while the remaining 27% of the phenomena are in the Liri-Garigliano basin (Fig. 2.2.4).
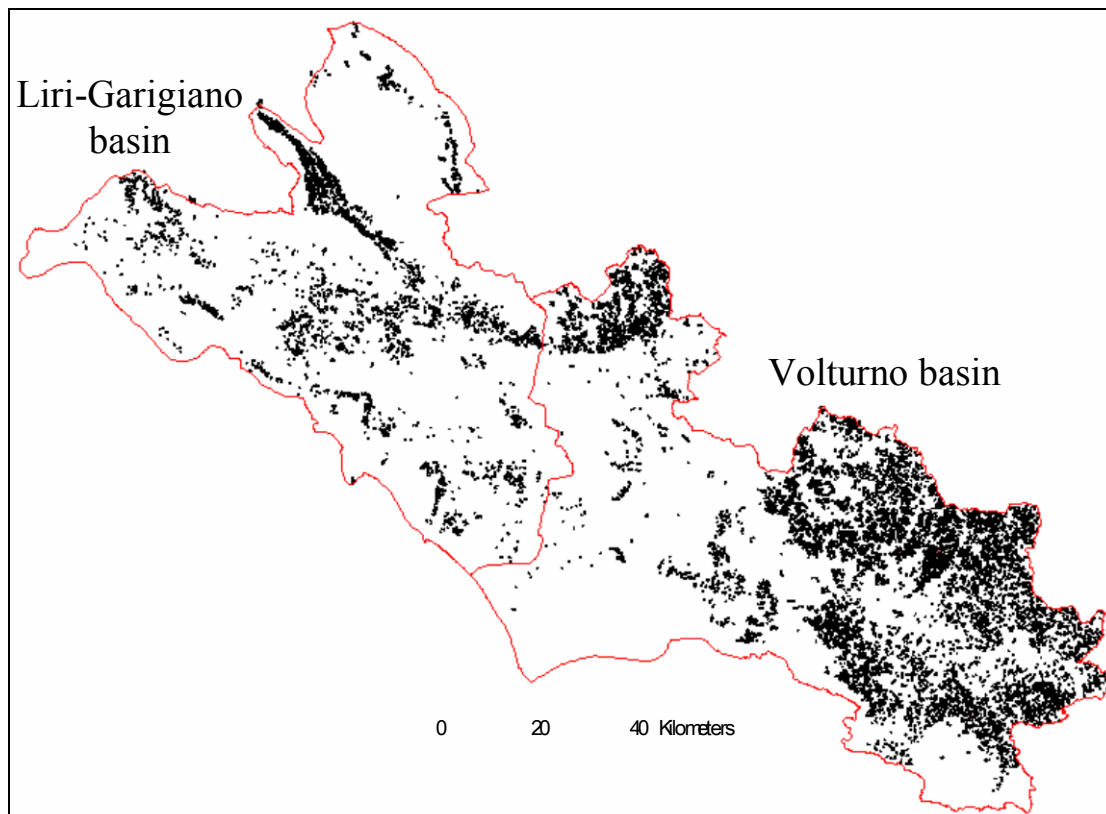
Figure 2.2.4 Slow-moving landslide inventory map of the territory of the National Basin Authority of "Liri-Garigliano and Volturno" rivers.

On the basis of the general framework shown in Figure 2.1.1, the role played by some predisposing factors in determining the spatial distribution of the existing slow-moving landslide within the territory was investigated. In particular, the studies carried out allowed the identification, through an index-based method (Soeters and van Westen, 1996; Coe et al., 2004), of the geo-lithological complexes most prone to slow-moving landslides, i.e. the areas in which more damages to facilities might be expected at a parity of built-up areas density. Then, further studies were carried out for the identification, within a given geo-lithological complex, of areas in which a different homogeneous "landsliding character" – in terms of both the existence or not of groups of phenomena and the shape/size of landslide-affected area (Pisciotta, 2008) – can be recognised (Fig. 2.2.5). This latter analysis was helpful to the definition of different vulnerability scenarios for municipalities located within homogenous contexts in terms of landsliding character, so overcoming the difficulties associated with the definition of landslide intensity at regional scale.
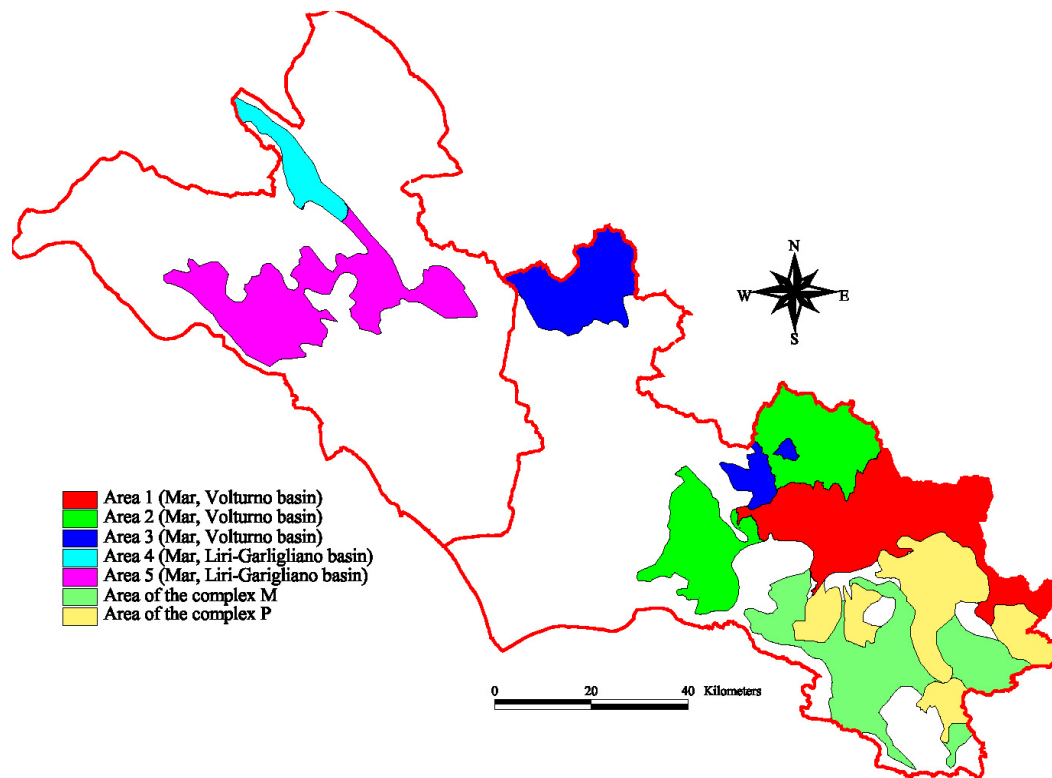
Deliverable D2.7   Rev. No: 1
Case studies of environmental and societal impact of landslides –
 Part A: Case studies for environmental (physical) vulnerability   Date: 2011-04-01

Figure 2.2.5 Map of the homogeneous areas with different "landsliding character".

The physical vulnerability at small scale, according to its definition, was estimated with reference to the territories of some municipalities (assumed as reference territorial units) chosen within three homogeneous areas (Areas 1, 2 and 3 in Figure 2.2.5) where the slow-moving landslide proneness is highest. The elements at risk, on the other hand, were considered as aggregates composed by three buildings, at least, according to the procedure adopted by the NBA LGV within the so-called Hydrogeological Setting Plan – Landslide risk excerpt (Italian Law 365/2000). The intersection of the building aggregates with the landslide-affected areas – mapped in the available landslide inventory map at 1:25,000 scale – allowed the detection of the vulnerable built-up areas falling within the municipal territories.

Once the vulnerable built-up areas were identified, physical vulnerability analyses were carried out thanks to the availability of the comprehensive database of landslide-induced damage furnished by the NBA-LGV; in particular, only damage whose severity affected the stability of the building superstructure (on the whole or a part of it) were considered for the analysis purposes. Then, considering that elements at risk were identified in terms of building aggregates, the concept of *"Equivalent Damage" (ED)* was introduced. In particular, for a given vulnerable area, ED is expressed by the formula:

$$ED = (N_0 \text{ of buildings with damage}) \text{ x } (Minimum \text{ building aggregation area}) \, [m^2]$$

where

Deliverable D2.7   Rev. No: 1
Case studies of environmental and societal impact of landslides –
 Part A: Case studies for environmental (physical) vulnerability   Date: 2011-04-01

N_0 of buildings with damage represents the number of damaged buildings within a vulnerable area

Minimum building aggregation area is considered equal to the area occupied by a buildings aggregation of three houses (1000 m^2 on the average, obtained by a check on the buildings aggregation within the study areas).

Finally, the physical vulnerability was estimated by a further Index, called "Areal Index of Damage" I_D, given by:

$$I_D = \frac{I_{VDU}}{I_{AVU}} = \frac{A_{AVD}}{A_{AV}} \cdot 100 \ [\%] \qquad\qquad [2.1]$$

In the above expression the Index I_{VDU} indicates the portion of urbanised areas, within a given municipality, potentially subjected to damage:

$$I_{AVU} = \frac{A_{AV}}{A_U} \cdot 100 \ [\%] \qquad\qquad [2.2]$$

where A_U is the whole urbanised area of a given municipal territory and A_{AV} is the whole urbanized area interacting with the landslides (i.e. the sum of the vulnerable areas); on the other hand, the Index I_{AVU} represents the vulnerable areas with damages related to the urbanised areas of a given municipality:

$$I_{VDU} = \frac{A_{AVD}}{A_U} \cdot 100 \ [\%] \qquad\qquad [2.3]$$

where A_{AVD} is the sum of the Equivalent Damages referring to the vulnerable areas with detected damages of a given municipal territory.

Finally, being the physical vulnerability defined in the SafeLand deliverable D2.5 as "*the ratio between the whole damageable vulnerable areas and the whole vulnerable areas of a given municipality*" vulnerability thresholds (V_{min} and V_{max}) were established, for each of the considered homogeneous areas, considering the curves respectively passing from the lowest and the highest value of the index I_D referred to the considered municipal territories (Galli and Guzzetti, 2007). An example is given in Figure 2.2.6 with reference to two municipal territories (chosen, respectively, for calibration and validation purposes) within the homogeneous area No. 1 where the presence of groups of large slow-moving landslides can be recognised (Pisciotta, 2008).

Once the vulnerability curves were calibrated and validated for each homogeneous geo-environmental context, the corresponding threshold values were used to predict the physical vulnerability of the built-up areas of municipal territories not included in calibration and validation analyses. Finally, the results were summarised in "Landslide vulnerability zoning maps" (Fig. 2.2.7) showing the spatial distribution of the minimum/maximum values of the expected degree of damage to the vulnerable areas of the municipal territories. It can be observed that the highest values of both minimum and maximum vulnerability concentrate in the Volturno river basin.

Deliverable D2.7
Case studies of environmental and societal impact of landslides –
 Part A: Case studies for environmental (physical) vulnerability

Rev. No: 1

Date: 2011-04-01
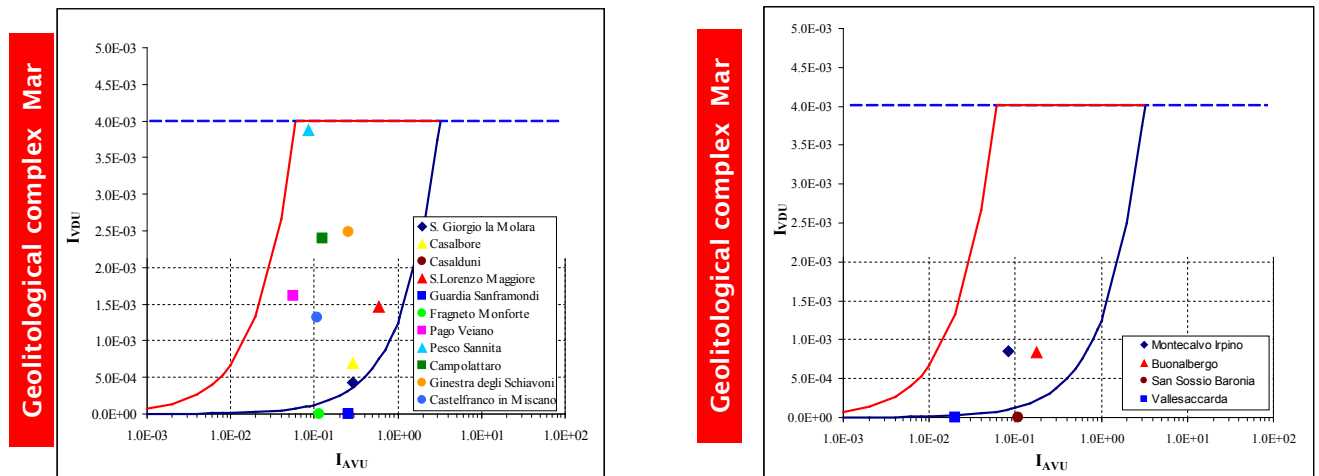
Figure 2.2.6 Physical landslide vulnerability curves referring to two samples of municipal territories - chosen, respectively, for calibration (a) and validation (b) purposes within the homogeneous area No. 1.

Maps similar to those obtained for the presented case study can be useful for the Authorities in charge of the land use planning and/or the disaster management planning. Moreover, they can represent a profitable tool for the engineers in evaluating possible constraints due to landslides in the development of large engineering projects.

Figure 2.2.7 Minimum (a) and maximum (b) landslide vulnerability zoning maps at small scale (1.100,000).

Deliverable D2.7   Rev. No: 1
Case studies of environmental and societal impact of landslides –
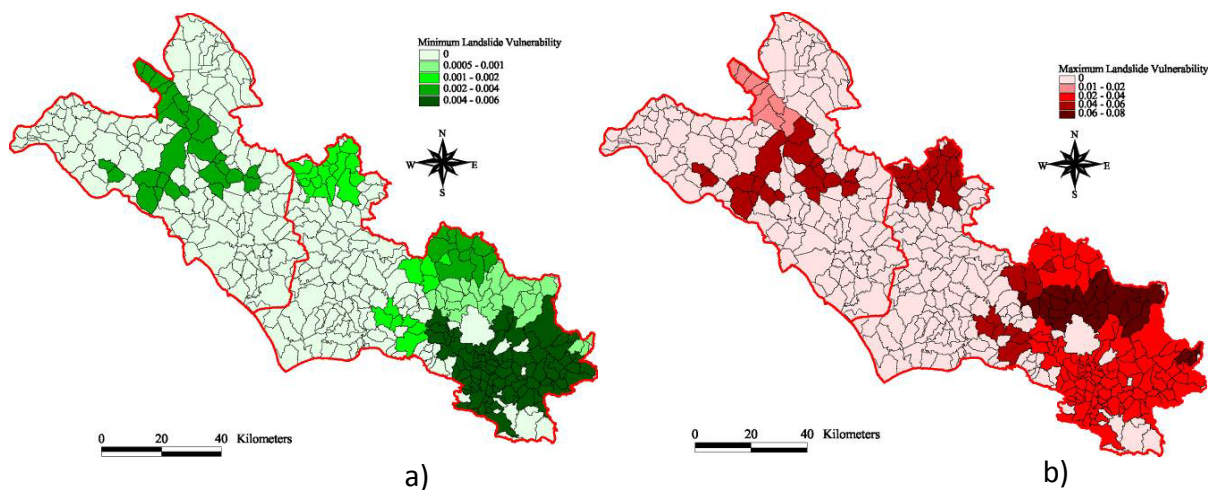 Part A: Case studies for environmental (physical) vulnerability   Date: 2011-04-01

3 APPLICATION TO BUILDING AGGREGATES AT TWO STUDY AREAS WITHIN THE TERRITORY OF THE NATIONAL BASIN AUTHORITY OF "LIRI-GARIGLIANO" AND "VOLTURNO" RIVERS, CENTRAL-SOUTHERN ITALY (SCALE: 1:25.000) (UNISA)

The physical vulnerability of smaller buildings aggregated units at two study areas (scale 1:25.000) within the territory investigated in Section 2 is estimated. A short review of the method is given in Subsection 6.1.

3.1 REVIEW OF THE METHOD

The procedure, described in SafeLand deliverable D2.5, Pitilakis et al. (2010) for the analysis of the physical vulnerability to slow-moving landslides at medium scale is based on a consequence model whose final product consists of vulnerability curves, i.e. the graphical relationship between the landslide intensity and the expected level of damage to a given buildings' aggregate. The followed methodological approach consists of sequential steps (Fig. 3.1.1).
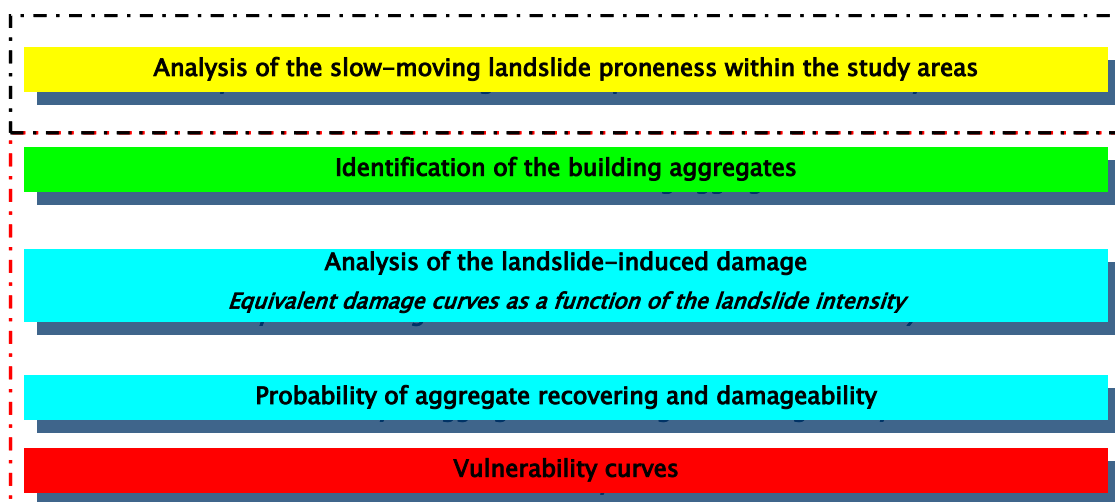
Figure 3.1.1 General framework for the physical vulnerability analysis at medium scale (modified from Viscardi 2010).

3.2 APPLICATION

In order to test the proposed procedure, two study areas belonging to the territory of the National Basin Authority of "Liri-Garigliano and Volturno" rivers were chosen (Fig. 3.2.1). These areas, in particular, are within the geo-lithological complexes most prone to slow-moving landslides, as recognised by studies carried out at regional scale (Pisciotta, 2008).
First of all, the analysis of spatial distribution of slow-moving phenomena within the study areas enabled the main landslide typology, the prevailing state of activity and some other characteristics of the phenomena censored (e.g. probability density distribution of landslide-

Deliverable D2.7   Rev. No: 1
Case studies of environmental and societal impact of landslides –
 Part A: Case studies for environmental (physical) vulnerability   Date: 2011-04-01

affected areas) to be identified. The obtained results were useful to justify the actual spatial distribution of both elements at risk and induced damages to the same elements.
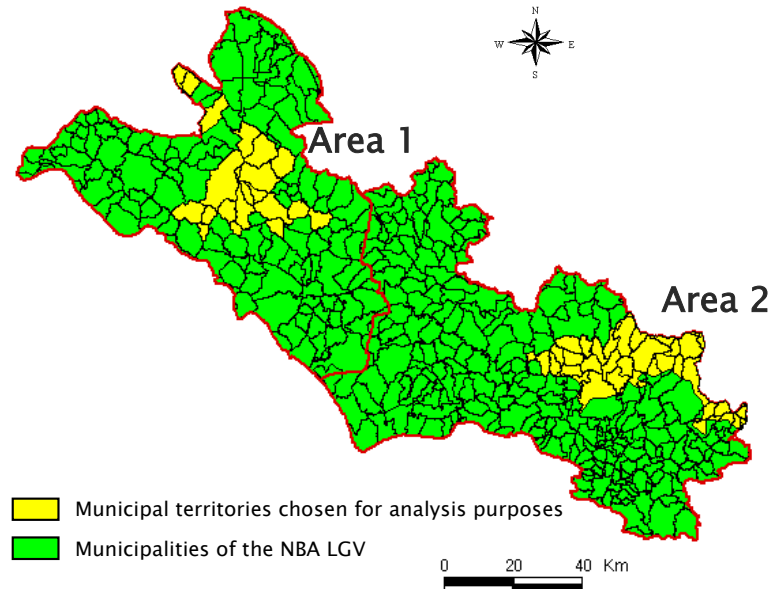
Figure 3.2.1 Study areas (1 and 2) selected within the territory of the National Basin Authority of "Liri-Garigliano and Volturno" rivers.

Once fixed the criteria for the identification of the elements at risk (Ferlisi and Pisciotta, 2007), the study was focused on the analysis of the distribution of damage to the vulnerable elements (building aggregates) in relation to their position within landslide-affected areas (i.e. at the head, in the main body, in the accumulation zone). The analysis was carried out by using the available dataset of landslide-induced damages to properties (Fig. 3.2.2) and introducing simplified schemes aimed to define the geometrical partition of the displaced mass depending on the landslide typology, namely: *i) rotational slide, ii) earthflow, iii) rotational slide–earthflow* (Cascini et al., 2010).

Deliverable D2.7
Case studies of environmental and societal impact of landslides –
 Part A: Case studies for environmental (physical) vulnerability

Rev. No: 1

Date: 2011-04-01

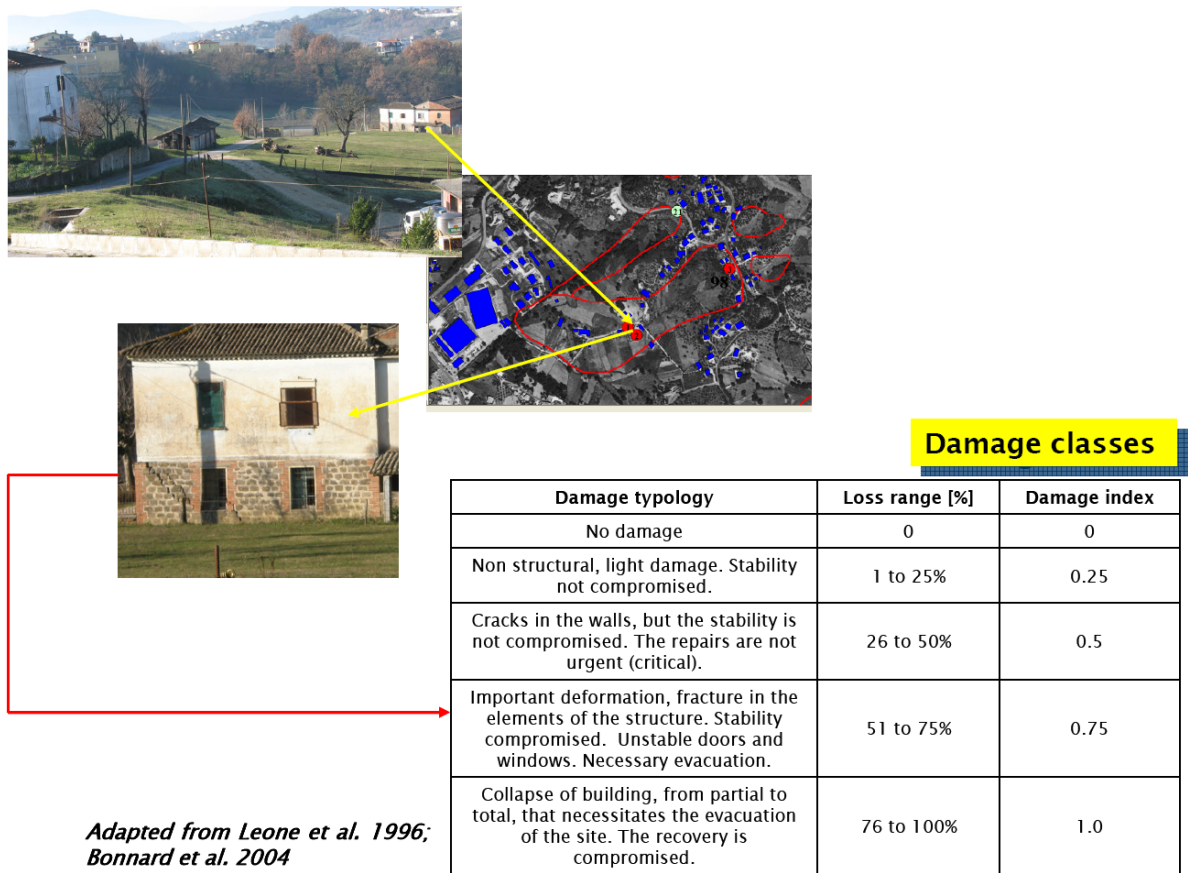| Damage typology	Loss range [%]	Damage index
No damage	0	0
Non structural, light damage. Stability not compromised.	1 to 25%	0.25
Cracks in the walls, but the stability is not compromised. The repairs are not urgent (critical).	26 to 50%	0.5
Important deformation, fracture in the elements of the structure. Stability compromised. Unstable doors and windows. Necessary evacuation.	51 to 75%	0.75
Collapse of building, from partial to total, that necessitates the evacuation of the site. The recovery is compromised.	76 to 100%	1.0

Adapted from Leone et al. 1996; Bonnard et al. 2004

Figure 3.2.2 Example of building damage recorded during field surveys and adopted damage classes.

The equivalent damage ED of a given vulnerable area was computed as the weighted average of the individual damage suffered by buildings belonging to areas affected by landslides. In general, the obtained results (Fig. 3.2.3) highlighted that the recorded damage severity is higher for vulnerable areas located at the head of the landslide body; moreover, the recorded damage to properties increase as the landslide-affected area increases.

Deliverable D2.7
Case studies of environmental and societal impact of landslides –
 Part A: Case studies for environmental (physical) vulnerability
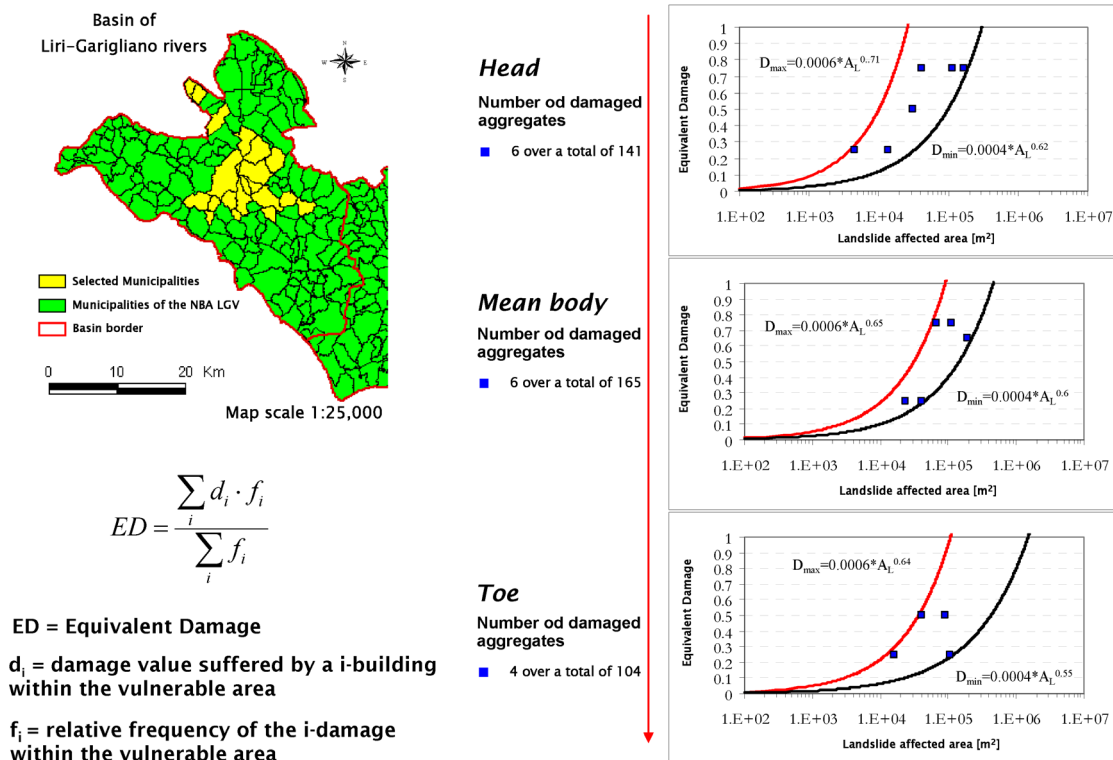
Rev. No: 1

Date: 2011-04-01

Figure 3.2.3 Example of Equivalent Damage curves obtained for building aggregates localised in different portions of the landslide bodies (study area of the Liri-Garigliano basin).

On the basis of its definition ("*the expected degree of damage to an aggregate, constituted by a given number of buildings, falling within an area affected by slow-moving landslides of a given intensity*"), the physical vulnerability was obtained by multiplying the Equivalent Damage times the spatial probability that a given aggregate interacts with a landslide times the probability that it suffers a given level of damage. Then, the results were finally used to obtain physical vulnerability curves (Fig. 3.2.4), similarly to the small scale. After a validation process, minimum and maximum values of the vulnerability, for a fixed landslide-affected area, were finally used for prediction purposes.
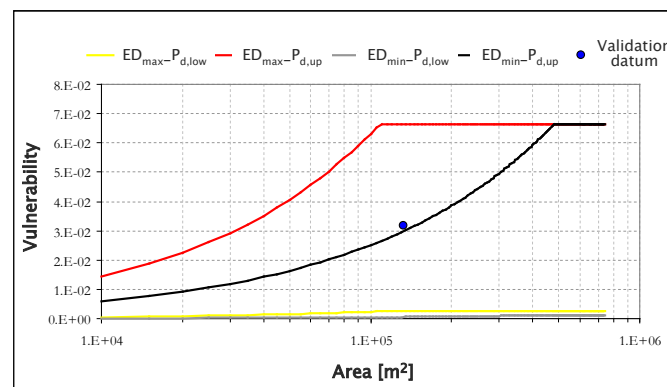

Figure 3.2.4 Example of vulnerability curves.

Deliverable D2.7   Rev. No: 1
Case studies of environmental and societal impact of landslides –
 Part A: Case studies for environmental (physical) vulnerability   Date: 2011-04-01

The final products of the analyses carried out are given by the physical minimum/maximum vulnerability zoning maps. An example of these maps is shown in Fig. 3.2.5 (numbers in the legends are dimensionless and time-independent; they indicate the probability that an aggregate may suffer a given level of damage depending on the number of buildings constituting the aggregate and the size of the landslide-affected area to which it interact).

It is worth noting that the vulnerability maps at medium scale can be useful in land use planning to select more suitable zones to be urbanised and to choose the alternative layouts of traffic facilities; moreover, they can be used to update the existing official maps made by River Basin Authorities within the "Hydrogeological Setting Plans" (Italian Law 365/2000).
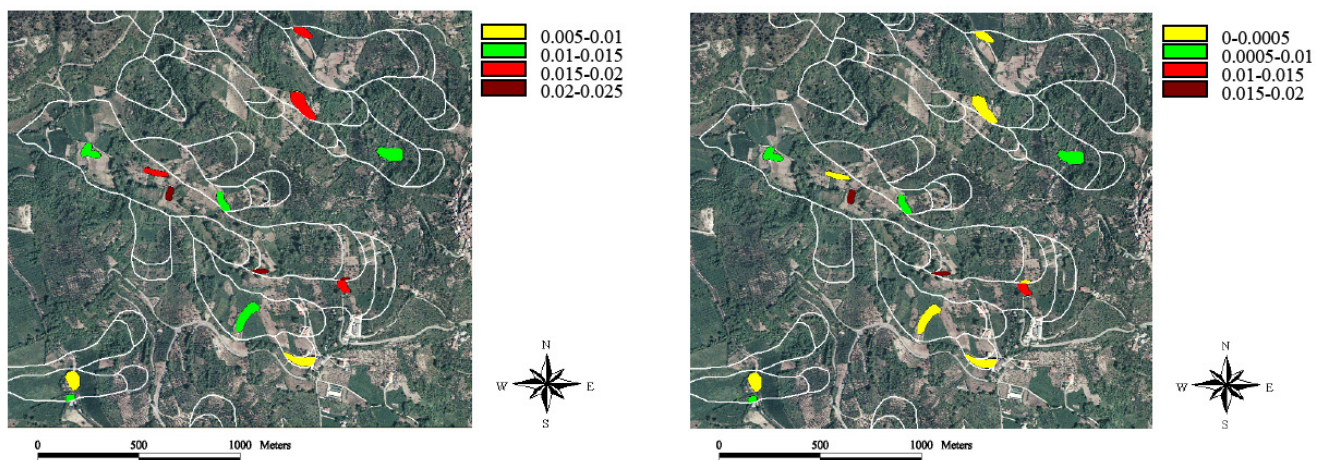
Figure 3.2.5 Minimum (a) and maximum (b) landslide vulnerability zoning maps at medium scale (1.25,000).

Deliverable D2.7   Rev. No: 1
Case studies of environmental and societal impact of landslides –
 Part A: Case studies for environmental (physical) vulnerability   Date: 2011-04-01

4   APPLICATION TO BUILDINGS LOCATED AT THE TEST SITE OF SAN PIETRO IN GUARANO, COSENZA PROVINCE, SOUTHERN ITALY (UNISA)

The physical vulnerability of buildings subjected to rainfall induced slow moving landslide hazard is assessed for the case of San Pietro test site in Guarano, Cosenza Province, southern Italy. The methodological framework is summerized in Subsection 6.1.

4.1   REVIEW OF THE METHOD

According to the contents of the SafeLand Deliverable D2.5, Pitilakis et al. (2010), the main goal of the analyses carried out at detailed scale consists of the physical vulnerability assessment by combining the results of numerical analyses with those deriving from the use of damageability criteria adopted in the geotechnical practice. In this regard, it can be observed that the reliability of the obtained results depends on: *i)* the quality of the input data to be used for the quantitative estimation of the parameters comparing in the adopted constitutive models or employed for the definition of the initial and boundary conditions of the problem at hand; *ii)* information achieved about the buildings at risk (in terms of their state of maintenance, structural typology of both superstructure and footing system, occupancy type, number of floors, etc.); *iii)* the completeness of the catalogue of damage data recorded to buildings after historical activation/reactivation of a given landslide displaced mass interacting with them.

A synthesis of the input data to be considered in order to characterise the landslide phenomenon and the elements at risk in activities aimed to the analysis and zoning of physical vulnerability at detailed scale is shown in Figure 4.1.1.
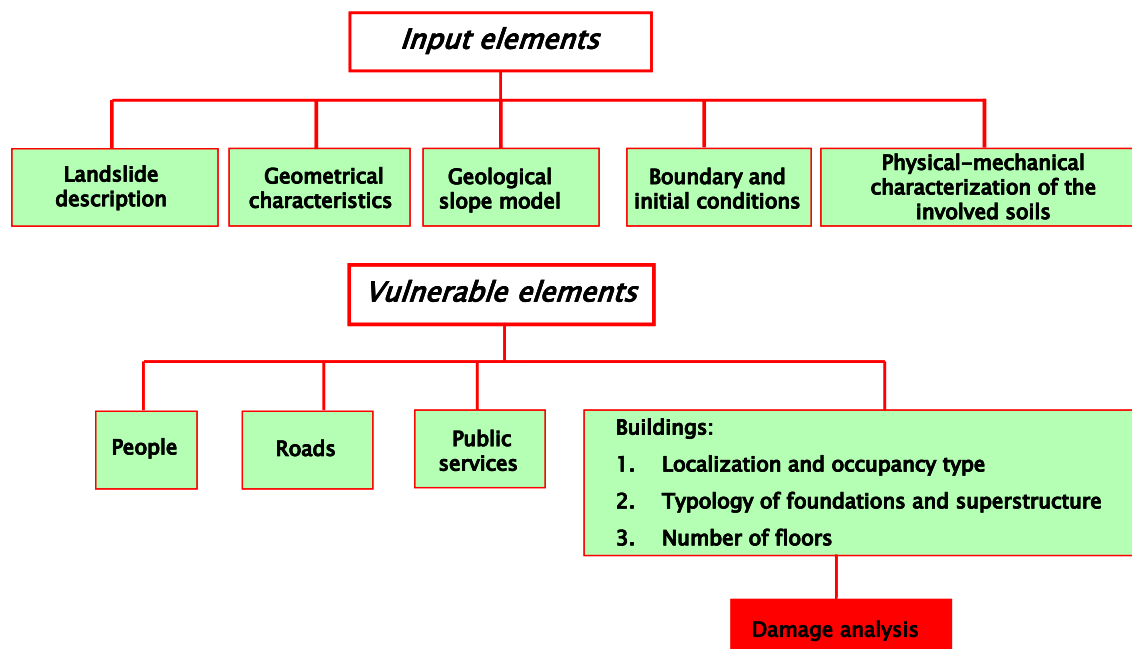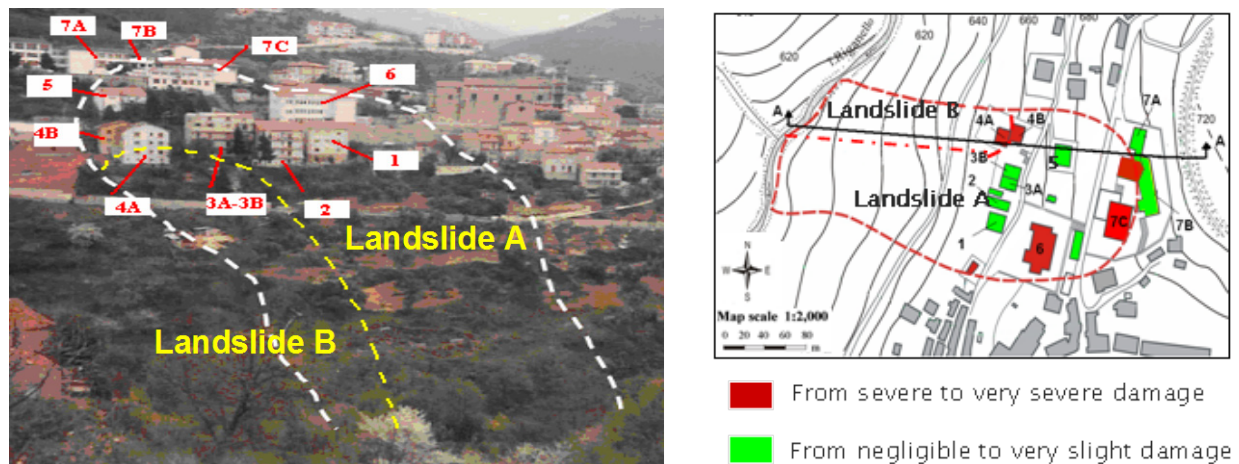

Figure 4.1.1 Input elements to be considered for the characterization of a landslide at detailed scale and data to be recorded about vulnerable elements.

Deliverable D2.7   Rev. No: 1
Case studies of environmental and societal impact of landslides –
 Part A: Case studies for environmental (physical) vulnerability   Date: 2011-04-01

4.2   SITE SPECIFIC APPLICATION

The procedure for the physical vulnerability analysis at detailed scale was applied to a landslide, in the municipal territory of San Pietro in Guarano (Cosenza Province, southern Italy), involving a subsoil formed by a gneissic cover filling in a paleogully (Cascini et al. 2006) and composed of two parts (Fig. 4.2.1a). During the last century, part B activated six times (1931, 1945, 1948, 1952/1953, 1976, 1981) in occasional and sudden reactivations that twice (1931, 1981) spread upslope, some hours later than the small landslide mobilization. Each event occurred during the wet season after intense cumulated rainfall and was characterised, within a short period of time (generally few hours), by small displacements not larger than few meters at the toe, and decreasing upslope. During the 1970s, after only two decades in dormant state, the landslide hazard was not recognised and many structures were built in the area. A schematic view of the buildings damaged during the last reactivation (January 1981) is shown in Figure 4.2.1b.

Figure 4.2.1 (a) Picture of the landslide-affected area and localization of the exposed buildings. (b) Planimetric view of the landslide-affected area and localization of the interacting buildings.

Some months after this reactivation a number of in situ and laboratory investigations were carried out for the landslide under study which extends over an urbanized area of about 20,000 m^2. In situ investigations consisted of drilling 28 boreholes, with a maximum depth of 70 m; collecting undisturbed and disturbed samples for laboratory determination of physical and mechanical properties; conducting in situ permeability tests; installing 46 piezometers (35 Casagrande piezometers and 11 open-pipe piezometers).

The in situ investigation and geological surveys indicated that, along the cross sections of the slope, the gneissic cover has a thickness ranging between 20 and 25 m. On the basis of the weathering-grade classification employed for the geological surveys, the cover is essentially composed of residual and saprolitic soils (classes VI and V), systematically including zones of colluvium and landslide debris, whose size ranges vary from a few decimetres to several metres. Following the geomorphological evidence, the landslide slip surfaces completely develop inside the cover, along a zone at the contact between the cover and the bedrock.

Deliverable D2.7   Rev. No: 1
Case studies of environmental and societal impact of landslides –
 Part A: Case studies for environmental (physical) vulnerability   Date: 2011-04-01

The bedrock is composed of highly to moderately weathered gneiss (class IV and III) and slightly weathered or fresh gneiss (class II and I) with fault gauge. It is characterised by a series of structural steps descending towards the foot of the slope, where a stream is slowly but permanently undermining the gneissic cover (Cascini et al., 1992).

Referring to the scheme proposed by Dietrich et al. (1982), the undermining action of the stream is considered the factor governing the slope response over geological periods of time. On the contrary, the reactivations over short periods of time (centuries) are connected to the increase in pore pressures induced both by rainfall and water inflows, the latter occurring in some zones along the structural discontinuity aligned with the buried paleogully. In this regard, according to Cascini and Versace (1988), the most critical rainfall events coincide with a cumulated daily rainfall of 900-1000 mm over a period of 100-110 days, with return periods of about 40-50 years.

The methodological approach followed in the conceived procedure includes two main steps (Viscardi, 2010). The first one deals with the development of numerical analyses devoted to: *i)* the simulation of the groundwater regime during rainfall event of given intensity and duration; *ii)* the detection of the mean values of the shear strength parameters mobilized along the shear zones; *iii)* FEM stress-strain analyses. The second step consists on the interpretation of the output data of the stress-strain analyses via the damageability criterion provided by Skempton and McDonald (1956).

As for the seepage simulations, the analyses were specifically devoted to find a relationship between rainfall and piezometric levels, systematically collected over about two decades. To this aim, rainfall, pore-pressure measurements and mechanical properties were analysed by using the Richards' differential equation, which provides the modelling of transient saturated – unsaturated water flow (Sorbino, 1994). By adopting this equation, the model was firstly calibrated referring to a period for which the piezometric measurements were available. Then, it was used to predict the groundwater table able to mobilise the slope, on the basis of the available rainfall data (Cascini et al., 2006).

Thanks to the recovered information about the groundwater critical level, it was possible to carry out the back-analyses devoted to obtain, via the use of Limit Equilibrium Methods, the values of the shear strength parameters mobilised at failure.

Finally, as it concerns the assessment of the displacements accumulated by the displaced body mass until its sudden reactivation, the results of FEM stress-strain analysis, performed using the SIGMA/W code (GEO-SLOPE, 2004) and considering all the data acquired via the previous analyses, are summarised in Figure 4.2.2 together with the consequence scenarios referring to cumulated rainfalls, respectively characterised by a return period of T = 50 years and T = 100 years.

Referring to the real return period (T = 50 years) of the landslide A, the analysis well explains the different damages recorded during the 1981 reactivation when building 4A-4B was completely destroyed and building 7A suffered slight consequences (Cascini, 1983). Indeed, according to the damageability criterion given by Skempton and McDonald (1956), the

Deliverable D2.7
Case studies of environmental and societal impact of landslides –
 Part A: Case studies for environmental (physical) vulnerability

Rev. No: 1

Date: 2011-04-01

relative rotation β attains, in correspondence of the portion topographic surface where building 4A-4B is located, a value exceeding the threshold (1/150) corresponding to the structural damage occurrence; on the contrary, the predicted β values in correspondence of the building 7a are lower than the recommended design value established by the Authors to prevent the damage occurrence.

However, when cumulated rainfall with T = 100 is considered, building 7A could suffer moderate damaged, as the relative rotation β attains values higher than the 1/300 threshold (in such a case, first cracking is likely to occur).
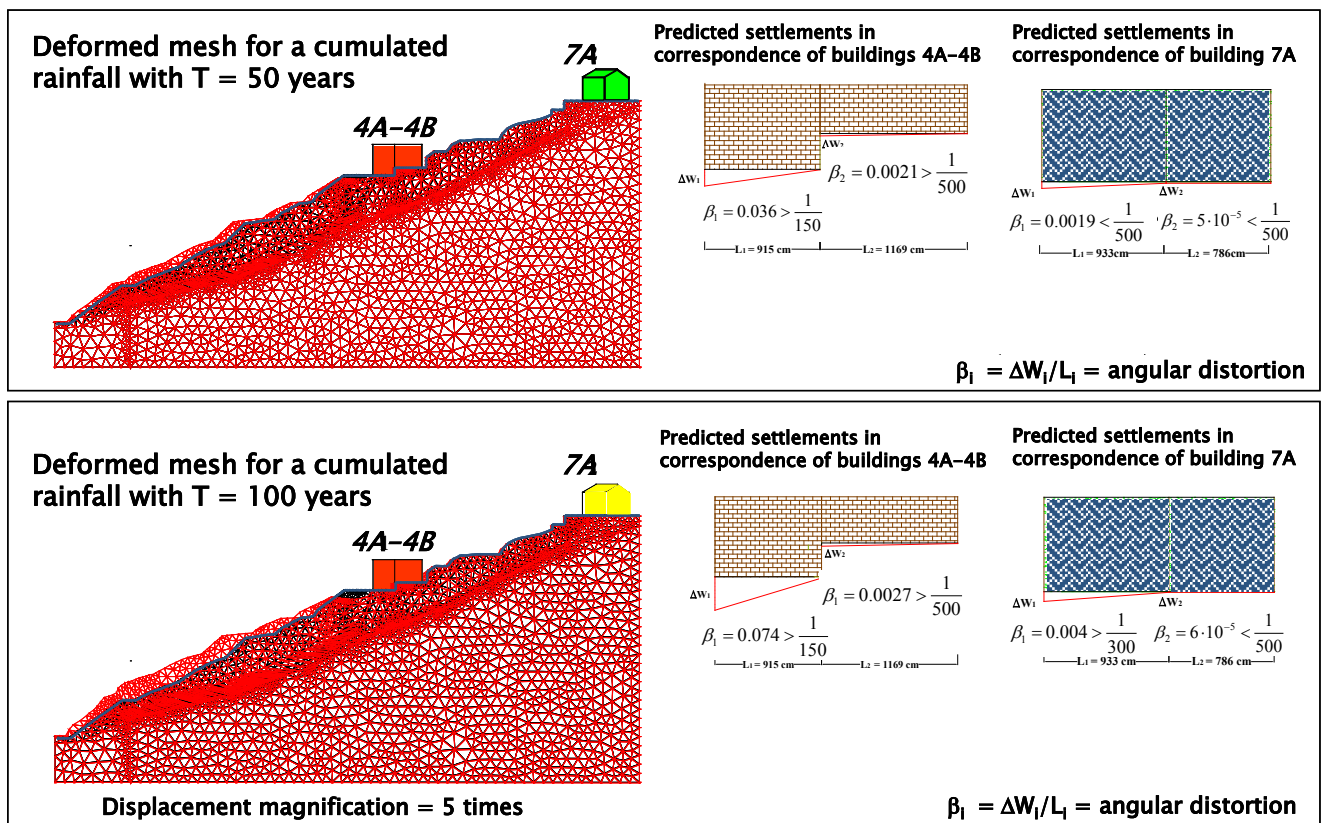

Figure 4.2.2 Consequence scenarios by FEM stress-strain analyses (modified from Cascini, 2008).

Deliverable D2.7   Rev. No: 1
Case studies of environmental and societal impact of landslides –
 Part A: Case studies for environmental (physical) vulnerability   Date: 2011-04-01

5 APPLICATION TO RC BUILDINGS LOCATED IN THE VICINITY OF KATO ACHAIA SLOPE, WESTERN GREECE (AUTH)

The physical vulnerability of RC buildings subjected to earthquake induced landslide hazard is assessed for the case of Kato Achaia slope in western Greece. The method is briefly reviewed in Subsection 6.1.

5.1 REVIEW OF THE METHOD

The proposed methodology, developed within the framework of Safeland -Deliverable D2.5, Pitilakis et al. (2010), Chapter 5.5 "Methodology for buildings at site specific scale (AUTH)", may be applied for assessing physical vulnerability of RC buildings due to earthquake triggered slow moving slides. It is principally based on a comprehensive set of numerical computations and statistical analysis. A brief description of the derived procedure is given herein.

A two-step uncoupled analysis is proposed: (a) estimation of differential permanent displacements (deformation demand) at the building's foundation level using an adequate finite difference dynamic slope model (b) statically application of the calculated differential displacements to building's model at the foundation level to assess the building's response for different ground landslide displacements induced by the earthquake. The computed permanent displacements at the foundation level were validated through comparison with simplified Newmark-type displacement methods. Structural limit states are defined in terms of a threshold value of building's material strain.

The complex issue of combined ground shaking and ground failure due to landslide is not taken into account in the evaluation of the building's vulnerability that is assessed only for effect of the permanent co-seismic displacement. In other words it is supposed that the oscillation of the building has no structural damages which may decrease the stiffness of the foundation and the building. In case of pre-landslide damages (seismic or other i.e. aging effects etc), these may be combined with the present damages through a general procedure which is under development.

The fragility curves as a function of PGA at the seismic bedrock were analytically derived via an extensive numerical parametric analysis considering different soil typologies, slopes geometries and building configurations and allowing explicit consideration of various sources of uncertainties.

5.2 SITE SPECIFIC APPLICATION

5.2.1 The Earthquake of 8 June 2008 in Achaia-Ilia, Greece

On 8 June 2008, a Mw 6.4 strong earthquake occurred in the area of northwest Peloponnese, western Greece, at a distance of about 17 km southwest of the town of Patras on a dextral strike slip fault (Figure 5.2.1). The main shock was recorded by 27 strong motion instruments at distances ranging approximately from 15 to 350 km from the surface projection of the fault (Margaris et al., 2010). Of those 27 stations, five that are within a relatively small region in Patras are shown in Figure 5.2.2. The event caused considerable structural damage to

Deliverable D2.7   Rev. No: 1
Case studies of environmental and societal impact of landslides –
 Part A: Case studies for environmental (physical) vulnerability   Date: 2011-04-01

buildings and infrastructures. Ground failure was widely observed within approximately 15 km of the fault, taking the form of landslides (mostly rockfalls), liquefaction, coastal subsidence, and settlement of fills (Margaris et al., 2008).

The town of Kato Achaia is located approximately 20 km from the epicenter of the main shock and from the town of Patras (Fig. 5.2.1). The minimum distance from the surface projection of the fault is estimated as Rjb = 6 km. The site along the coast of Kato Achaia was found to suffer extensive ground deformation due to liquefaction. However, it is not our objective here to study liquefaction phenomena. Preliminary investigation on Kato Achaia area indicates peak horizontal ground acceleration values on the **order of 0.3g**, quite higher than the values recorded in Patras downtown.
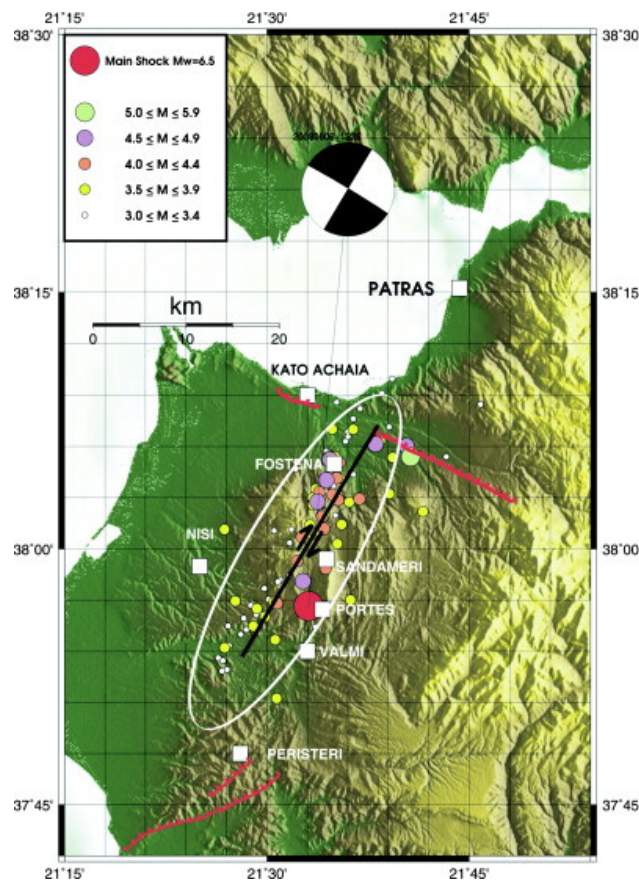
Figure 5.2.1 Fault of the June 8, 2008 sequence (black) (determined by analysis of the main shock and aftershock distribution) and already mapped faults (red).The red circle denotes the epicenter of the main shock. Towns affected by the earthquake are denoted by squares. (Margaris et al. 2010).

An important concentration of severe building damages is observed near the edge of the cliff that comprises the northern boundary of Kato Achaia town (Figure 5.2.3). This is probably due to simple site amplification in the vicinity of the crest as it is illustrated by the amplification of the horizontal acceleration and the generation of parasitic vertical acceleration near the top of the slope (Athanasopoulos G. and Pefani H., personal communication, 2010). However such models are not considering any effect from permanent ground displacements due to differential ground movements close to the slope and the crest. In the present we are investigating the possible presence of both phenomena.
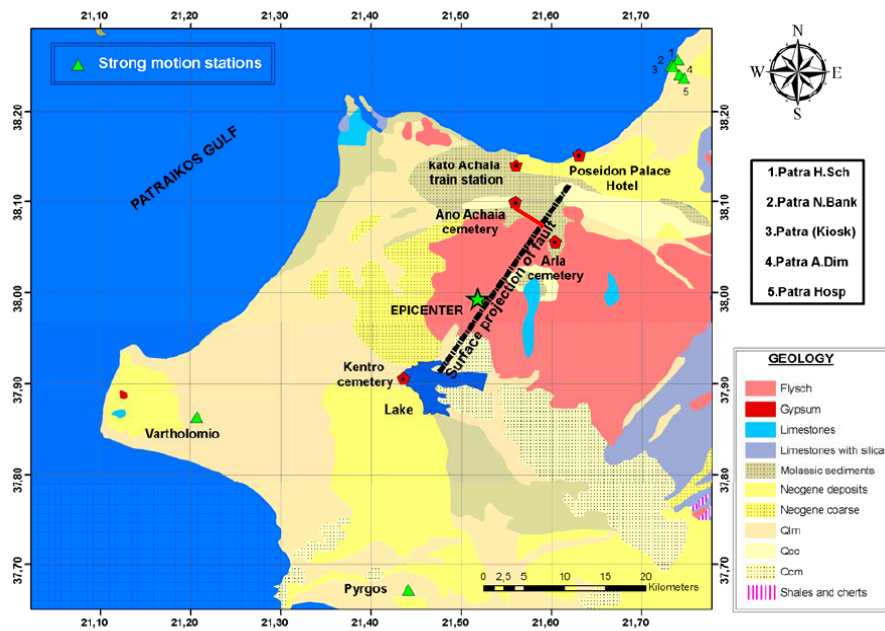
Deliverable D2.7
Case studies of environmental and societal impact of landslides –
 Part A: Case studies for environmental (physical) vulnerability

Rev. No: 1

Date: 2011-04-01

Figure 5.2.2 Strong motion stations located near the ruptured fault segment. Distance of Kato Achaia town from the surface projection of the fault.

Figure 5.2.3 denotes the area with the larger concentration of damaged buildings (in red), while the narrow red zone indicates the area with complete collapses of the buildings. As expected for this level of shaking, the field reconnaissance survey revealed that the earthquake did not cause the complete failure of the slope; only minor permanent deformations were observed at the slope's crown, implying that the building damage occurred primarily as a result of ground shaking and its amplification due to the topographic and complex site effects and not in consequence of extensive co- seismic irreversible slope deformation. However this has to be confirmed through numerical non-linear analysis.
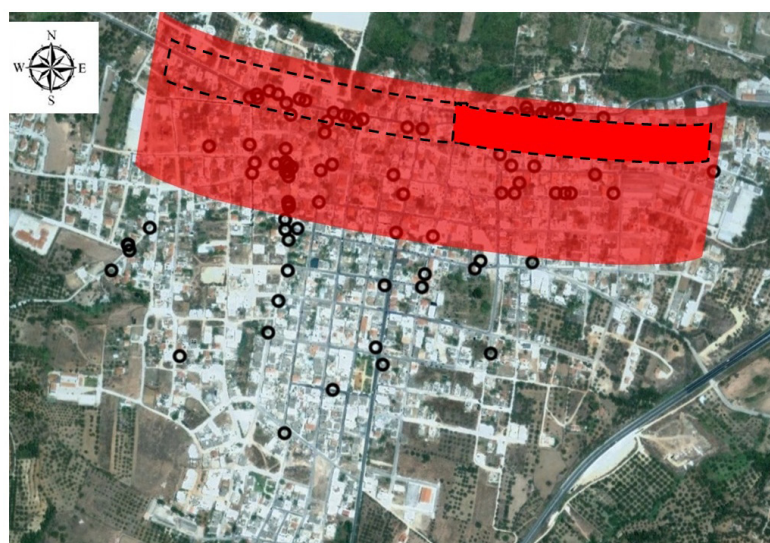

Figure 5.2.3 Geographical distribution of the buildings (black circles) suffered severe damage in Kato Achaia

Deliverable D2.7   Rev. No: 1
Case studies of environmental and societal impact of landslides –
 Part A: Case studies for environmental (physical) vulnerability   Date: 2011-04-01

5.2.2   Slope non-linear dynamic analysis

The present study aims at the investigation through numerical fully non-linear dynamic analysis of the Kato Achaia slope performance and the potential effects on the buildings located in the vicinity of the slope's crest; we examine different earthquake hazard scenarios.
The main idea is firstly to verify through numerical nonlinear constitutive models that for the 8 June 2008 earthquake the observed building damages occurred primary as a result of amplified ground shaking; then, for a stronger earthquake hazard scenario (e.g. with a mean return period Tm of 1000 years), we are proposing to assess the vulnerability due to permanent co-seismic slope displacement of an assumed RC building standing near the slope's crown. More specifically, the analytical methodology developed in Folopoulou et al. (2011) and improved in Fotopoulou and Pitilakis (2011) for the vulnerability assessment of RC buildings subject to earthquake induced slow moving slides is used.
In order to estimate structural vulnerability for a given earthquake triggered landslide scenario, one could directly use the fragility curves derived via numerical parametric analysis in SafeLand, D2.5 (Chapter 5.5), Pitilakis et al. (2010). These correspond to the simplified geometrical, geological and structural settings for the slope and the structure. Nevertheless, it was decided to reproduce the numerical simulation for the real slope geometrical, hydro-geotechnical, geological and shaking characteristics to check the reliability and applicability band of the proposed simplified curves.
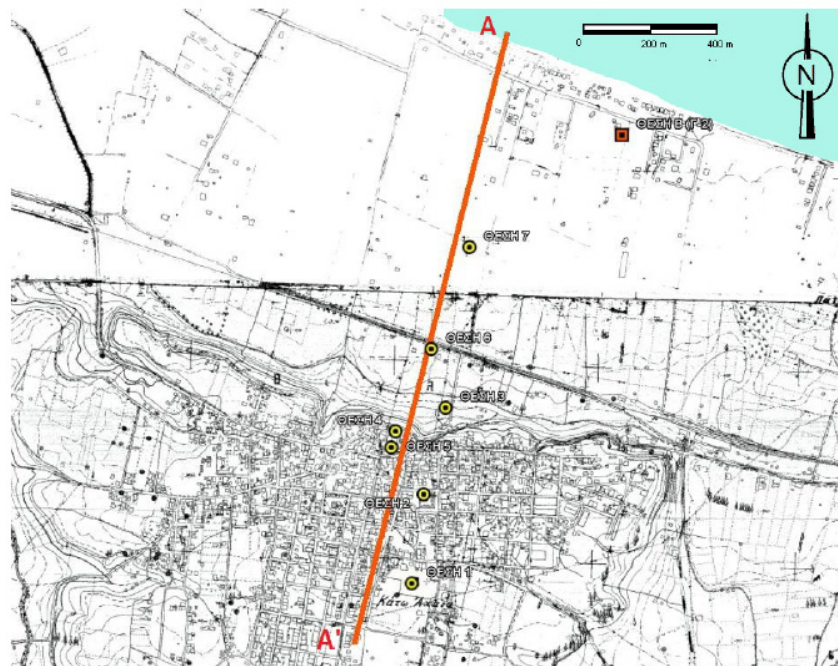
*Figure 5.2.4 Topographic map (original scale 1:5000) of Kato Achaia area and position of A-A'
cross section.*

Figure 5.2.4 presents the topographic map (original scale 1:5000) of the Kato Achaia area and the location of the 2 dimensional cross-section A-A' used to conduct the numerical dynamic analysis. A geotechnical and geophysical investigation has been performed by the University

Deliverable D2.7
Case studies of environmental and societal impact of landslides –
 Part A: Case studies for environmental (physical) vulnerability

Rev. No: 1

Date: 2011-04-01

of Partas (Greece) Civil Enginnering Department (UPatras; http://www.civil.upatras.gr/) in the broader area including geotechnical boreholes, N_{SPT} tests, Surface Waves tests (using ReMi, SASW and MASW techniques) and classical geotechnical laboratory tests on representative and undisturbed soil samples. Based on the above data provided by the University of Patras, Fig. 5.2.5 (a) presents the simplified 2-dimensional cross-section used for the dynamic analysis together with the (two) sites of geotechnical boreholes and the profile of low-strain shear wave velocity, V_S, of the slope area. The water table is found to be located 30 m above the slope's crest and 1m above the slope's toe. The geotechnical surveys reveal 9 different soil layers (Fig. 5.2.5(b)). The geotechnical characteristics assigned to each layer are summarized in Table 5.2.1. It should be noted that the investigation of the potential for liquefaction is beyond the scope of this study.

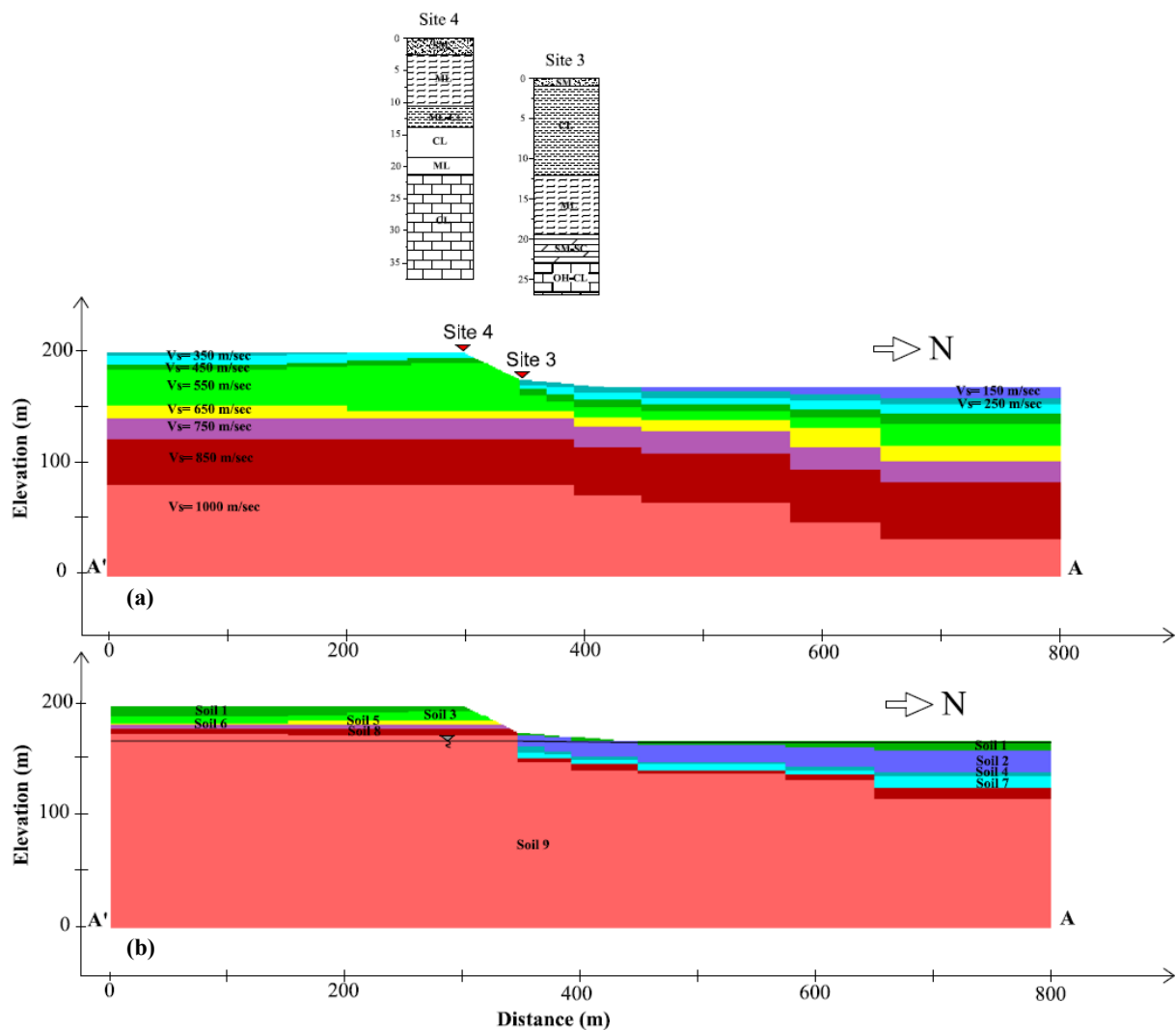*Figure 5.2.5 Soil model used for the 2D finite difference dynamic analysis*

In order to establish correlation between the earthquake demand and the permanent differential displacements for the building, dynamic non-linear analyses were performed using the computer code FLAC 5.0 (Itasca, 2005). The soil materials are modeled using an elastoplastic constitutive model with the Mohr-Coulomb failure criterion, assuming a zero

Deliverable D2.7   Rev. No: 1
Case studies of environmental and societal impact of landslides –
 Part A: Case studies for environmental (physical) vulnerability   Date: 2011-04-01

dilatancy non-associated flow rule. The discretization allows for a maximum frequency of at least 10Hz to propagate through the finite difference grid without distortion. A small amount of mass- and stiffness-proportional Rayleigh damping is also applied (0.5-2%), to account for the energy dissipation in the elastic range. The center frequency of the installed Rayleigh damping is selected to lie between the fundamental frequencies of the input acceleration time histories and the natural modes of the system. The 2D dynamic model is 800m wide and the elevations of ground surface vary from 160 to 195 m. The slope's height and inclination are estimated at 23 m and 28° respectively.

Table 5.2.1 Soil properties

Material	γ_d (KN/m^3)	γ_{sat} (KN/m^3)	Poisson's ratio	Vs (m/sec)	Friction angle (degrees)	Cohesion (KPa)
Soil 1 (SM-CL)	18	20	0.4	150-250	27	5
Soil 2 (CL)	19	21	0.4	250-450	20	35
Soil 3 (ML)	19	21	0.4	450-550	34	5
Soil 4 (ML)	19	21	0.4	450-550	38	5
Soil 5 (CL-ML)	20	21	0.4	450-550	30	8
Soil 6 (ML)	20	21	0.4	550	24	15
Soil 7 (SM-SC)	20	21	0.4	550	40	8
Soil 8 (OL-CL-OH)	20	21	0.4	550	22	50
Soil 9 (OL-CL)	21	22	0.4	550-1000	28	80

Free field absorbing boundaries are applied along the lateral boundaries while quiet (viscous) boundaries are applied along the bottom of the dynamic model to minimize the affect of reflected waves. In order to apply a compliant base along the same boundary as the dynamic input, the seismic motions must be input as stress loads combining with the quiet (absorbing) boundary condition.

A RC building is assumed to be located 3m from the slope's crest. The building is modeled only by its foundation with a width of 6m (uncoupled approach). A flexible foundation system (isolated footings) simulated with concentrated loads (P=50KN/m) at the footings' links is considered. Thus, no relative slip between foundation and subsoil is permitted.

Due to the lack of acceleration records within the slope area, two different strong motion time-histories recorded at the stations PAT3 – (Patra High School) and Pat_Hosp (Patra Hospital) of the town of Patras were used in the numerical simulations (see Figure 5.2.2). The base motions imposed in the dynamic model were obtained by deconvolution of the motion recorded in Patras and appropriate scaling for distance. The code Cyberquake (BRGM Software 1998) and the profiles of Fig. 5.2.6 were used for this purpose. Site conditions for the selected stations were made available from previous geotechnical and geophysical investigations (Athanasopoulos G. and Pefani H., personal communication, 2010). Three different sets of G-γ-D curves proposed by Darendeli (2001), which account for soil plasticity, OCR, and overburden pressure, were used for the deconvolution analysis (Fig. 5.2.6). The deconvoluted excitations which were obtained and used as seismic input are shown in figure 5.2.7. Before applied to our Kato Achaia 2D the model, they are subjected to appropriate correction (baseline correction and filtering) to allow for an accurate representation of wave transmission through the model.

Deliverable D2.7
Case studies of environmental and societal impact of landslides –
 Part A: Case studies for environmental (physical) vulnerability
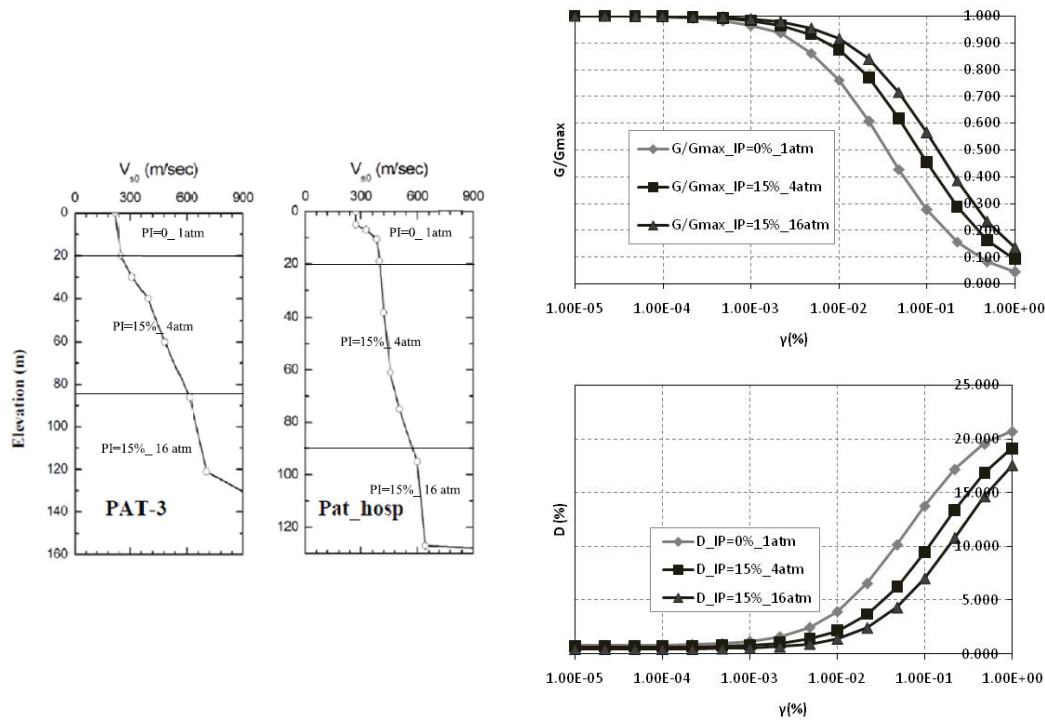
Rev. No: 1

Date: 2011-04-01

*Figure 5.2.6 Shear wave velocity variation with depth for the selected recording stations (left).
Modulus reduction and damping curves of Darendeli (2001) used for the 1D deconvolution analysis
(right).*

Finally the input accelerograms are scaled to two levels of peak ground acceleration at the assumed seismic bedrock, namely PGA_{base}= 0.2 and 0.5g. The low level of excitation is taken to be consistent with the PGA values reported at the Kato Achaia area during the 2008 Ilia Achaia earthquake (reaching PGA values on the order of 0.3g at the free surface). The higher excitation level (PGA=0.5 g) is considered in order to further investigate irreversible deformation beneath the building's foundation and finally to assess the vulnerability of the assumed building due to the differential permanent ground displacement induced by the landslide. The differential horizontal ground displacements at the foundation level derived from the 2D finite difference dynamic analysis by applying the PAT3-T and Pat_hosp-N accererograms at the assumed seismic bedrock are schematically illustrated in Figure 5.2.8 for the two levels of excitation.
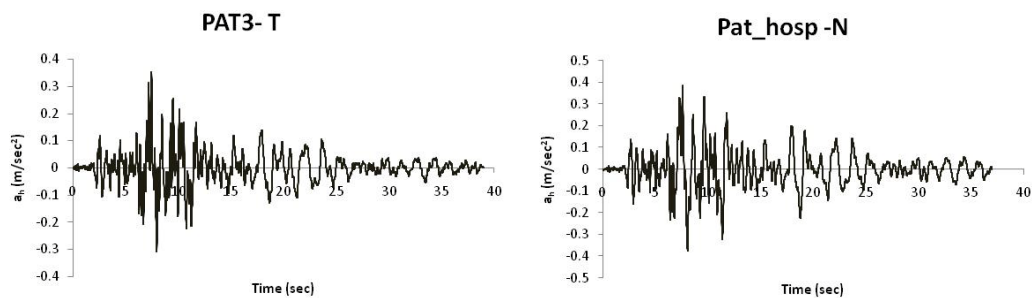

Figure 5.2.7 Input outcropping horizontal accelerations used in the dynamic analysis

Deliverable D2.7   Rev. No: 1
Case studies of environmental and societal impact of landslides –
 Part A: Case studies for environmental (physical) vulnerability   Date: 2011-04-01

In accordance with the field observations carried out after the 2008 Achaia-Ilia earthquake, quite small (<10cm) total and differential deformations at the building's foundation level are anticipated when applying the outcropping horizontal accelerograms scaled at PGA_{base}=0.2g (Fig. 5.2.8 left). In contrast, for the stronger earthquake scenario (PGA_{base}=0.5g), remarkable differential permanent displacements (0.4m - 0.6m) are expected (fig 5.2.8 right).
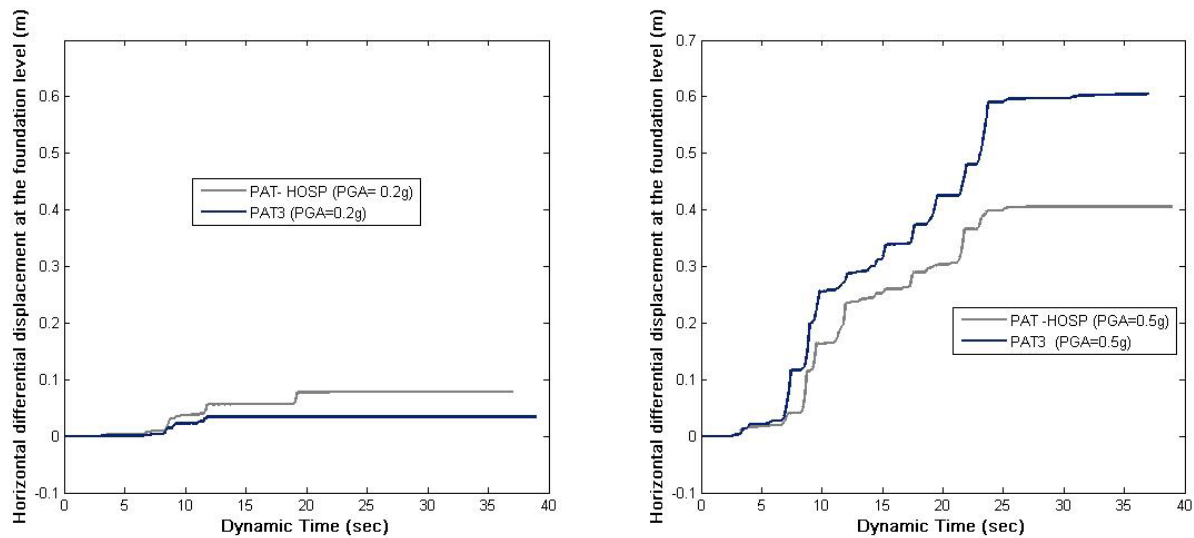

Figure 5.2.8 Differential horizontal ground displacements at the building's foundation level for low (left) and high (right) excitation level.

5.2.3   Fragility analysis of the building

The analysis of the building is conducted by means of the finite element code SeismoStruct (Seismosoft, 2007), which is capable of calculating the large displacement behavior of space frames under static or dynamic loading, taking into account both geometric nonlinearities and material inelasticity. Both local (beam-column effect) and global (large displacements/rotations effects) sources of geometric nonlinearity are automatically taken into account. The spread of material inelasticity along the member length and across the section area is represented through the employment of a fiber-based modeling approach, implicit in the formulation of SeismoStruct's inelastic beam-column frame elements. Nonlinear static time-history analyses are performed for all numerical simulations. In particular, the differential permanent displacement (versus time) curves (Fig. 5.2.8), directly extracted from the FLAC dynamic analysis, are statically imposed at one of the RC frame supports.
The studied building is a "low code" single bay-single storey RC bare frame structure, considering that most of the existing RC buildings found in the area are low rise, old, poorly constructed structures. The building's height and length are 3m and 6m respectively. A uni-axial nonlinear constant confinement model is used for the concrete material (fc=20MPa, ft=2.1MPa, strain at peak stress 0.002mm/mm, confinement factor 1.2), assuming a constant confining pressure throughout the entire stress-strain range (Mander et al, 1988). For the reinforcement, a uni-axial bilinear stress-strain model with kinematic strain hardening is utilized (fy=400MPa, E=200GPa, strain hardening parameter μ =0.005). All columns and

Deliverable D2.7
Case studies of environmental and societal impact of landslides –
 Part A: Case studies for environmental (physical) vulnerability

Rev. No: 1

Date: 2011-04-01

beams have rectangular cross sections (0.40x 0.40m). A low level of steel reinforcement is used (8Φ12) for all the cross sections considered.

The building structural response is obtained for the two different levels of excitation by analyzing the building capacity under the deformation demand. In order to identify the building performance (damage) state, 4 limit states (LS1, LS2, LS3, LS4) are defined, based on the work of Crowley et al. (2004), Bird et al. (2005) and engineering judgment (Table 5.2.2). These concern exceedance of minor, moderate, extensive and complete damage of the building.

Table 5.2.2 Definition of Limit states for "low code" RC buildings

Limit state	Steel strain (ε_s) –low code design
LS1	Steel bar yielding
LS2	0.0125
LS3	0.025
LS4	0.045

The building's damage level is finally assessed by comparing the response of the critical member of the building (in terms of maximum steel strain) for the given hazard level to the specified threshold values for each limit state.

As expected, the building will sustain slight damage (maximum steel strain at the critical column $\varepsilon_{s,ave}$ =0.0027) due to permanent ground deformation (landslide) for the low level of input excitation (PGA=0.2g) which most probably happened during the earthquake under consideration. This is in line with the minor permanent slope displacement observed after the 2008 Achaia-Ilia earthquake. On the contrary, for the strong earthquake scenario (PGA=0.5g), the structure is expected to suffer complete damage (maximum steel strain at the critical column $\varepsilon_{s,ave}$ =0.0545), making the repair of the building non feasible in physical or economical terms.
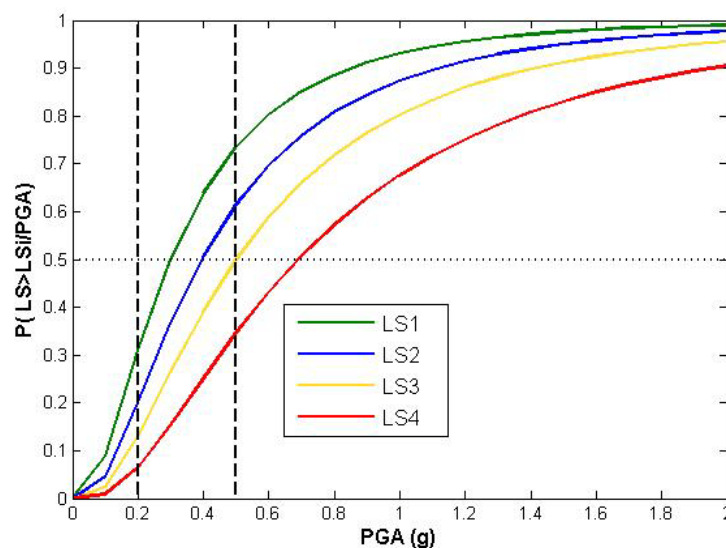

Figure 5.2.9 Fragility curves proposed for the specific site and structural characteristics

Deliverable D2.7
Case studies of environmental and societal impact of landslides –
Part A: Case studies for environmental (physical) vulnerability

Rev. No: 1

Date: 2011-04-01

Conclusive remarks:

The fragility curves developed in Safeland-Deliverable 2.5, Pitilakis et al. (2010) that are found to be more representative of the geotechnical, geological, geometrical and structural characteristics of the site and the building are depicted in Figure 5.2.9. It is seen that the proposed curves predict that the typical building studied herein would suffer extensive damage (worst probable damage state/ i.e. exceeding probability >50%) for the high seismic hazard scenario (PGA_{base}=0.5g) and no or low damage for the low seismic hazard scenario (PGA_{base}=0.2g). These observations are in good agreement with the observed (for the low hazard scenario) and computed damages (for both hazard levels) of the typical building, considering also the high variability associated with the curves (standard deviation of the natural logarithm of PGA, βi, on the order of 0.8).

Hence, it is concluded that the proposed fragility curves despite their simplifications seem to adequately capture the performance of the RC building affected by the slope co-seismic landslide differential displacement.

Deliverable D2.7   Rev. No: 1
Case studies of environmental and societal impact of landslides –
 Part A: Case studies for environmental (physical) vulnerability   Date: 2011-04-01

6   APPLICATION TO THE ROADWAY SYSTEM OF GREVENA CITY, GREECE   (AUTH)

The physical vulnerability of roads due to landslide hazard is assessed for the broader urban area of Grevena city in Greece. The method is briefly reviewed in Subsection 6.1. It is noted that the same area is used as a case study for the societal vulnerability approach (see part B of the present report).

6.1   REVIEW OF THE METHOD

The proposed method developed within the framework of Safeland -Deliverable D2.5, Pitilakis et al. (2010), Chapter 5.7 "Methodology for roads (AUTH)", may be applied to assess the vulnerability of roads subject to earthquake triggered landslides. It is based on a modification of the existing HAZUS fragility curves using the Bray and Travasarou (2007) model (eq. 6.1) that relates the seismic permanent ground displacement (D) with the peak ground acceleration (PGA) for the Newmark rigid sliding block case (*Ts*=0). In this respect, it is possible to include the specific characteristics of soil and local topography within the definition of road vulnerability. The derived fragility curves are given as a function of PGA considering the characteristics of the slope (i.e. yield coefficient, k_y).

$$\ln(D) = -0.22 - 2.83 \ln(k_y) - 0.333 (\ln(k_y))^2 + 0.566 \ln(k_y) \ln(PGA)$$
$$+ 3.04 \ln(PGA) - 0.244(\ln(PGA))^2 + 0.278(M-7) \pm \varepsilon \qquad \text{[6.1]}$$

where,
PGA: peak ground acceleration of the ground motion (i.e., $S_a(Ts=0)$);
D: seismic ground displacement;
ky: yield coefficient.

In particular, using the existing HAZUS fragility curves, the exceedance probabilities of each damage state are calculated for the corresponding PGD values that are derived for a range of PGA values based on the aforementioned relationship. Then a lognormal distribution is fitted on each curve and the median and standard deviation parameters (β) are estimated for a given yield coefficient, earthquake magnitude and damage state.

6.2   APPLICATION AND RESULTS

Grevena is a town and municipality in Greece, capital of the Grevena Prefecture located on the NW part of Greece (Fig. 6.2.1). The city is surrounded by mountains, while is situated by the river Greveniotikos, which itself flows into the main river Aliakmon. Consequently the landslide risk during a strong earthquake may be quite important.

Deliverable D2.7   Rev. No: 1
Case studies of environmental and societal impact of landslides –
 Part A: Case studies for environmental (physical) vulnerability   Date: 2011-04-01

Figure 6.2.1 *Location of the city of Grevena in Greece*

The seismic vulnerability of the roadway system of Grevena has been investigated in previous project using the HAZUS (NIBS, 2004) multi-hazard methodology. The results revealed that most of the expected damages are attributed to the occurrence of permanent ground deformations due to landsliding and not to the effect of ground shaking (Pitilakis et al., 2009; Pitilakis et al. 2011). The total length of the road network under study is approximately 19.68 km.

Critical accelerations for landsliding were estimated as a function of local soil conditions and topography using the HAZUS simplified methodology. They were found to vary from 0.1 to 0.3g for slope angles between 5° and 90°. The expected PGA values at the free ground surface were derived from the results of the microzonation study of the area for three seismic scenarios that refer to earthquakes with mean return periods of 100, 500 and 1000 years (Pitilakis et al., 2009; Pitilakis et al. 2011).

Based on the deaggregation of seismic hazard, the most likely earthquake moment magnitude and source-site distance for three mean return periods (T_m=100, 500 and 1000 years), and two soil conditions (B and C according to EC8) were estimated. For example, the 500 years scenario corresponds to a 6.3 earthquake with R=14km for soil type B and R=13km for soil type C.

For the vulnerability assessment of the roadway system of Grevena, the fragility curves proposed for roads with two traffic lanes (urban roads) are used (Fig. 6.2.2). The estimated medians and dispersions of these fragility curves for each damage state and yield coefficient are presented in Table 6.2.1.

Deliverable D2.7
Case studies of environmental and societal impact of landslides –
Part A: Case studies for environmental (physical) vulnerability

Rev. No: 1

Date: 2011-04-01

Table 6.2.1   Fragility parameters for urban roads on slope for M=6.3.

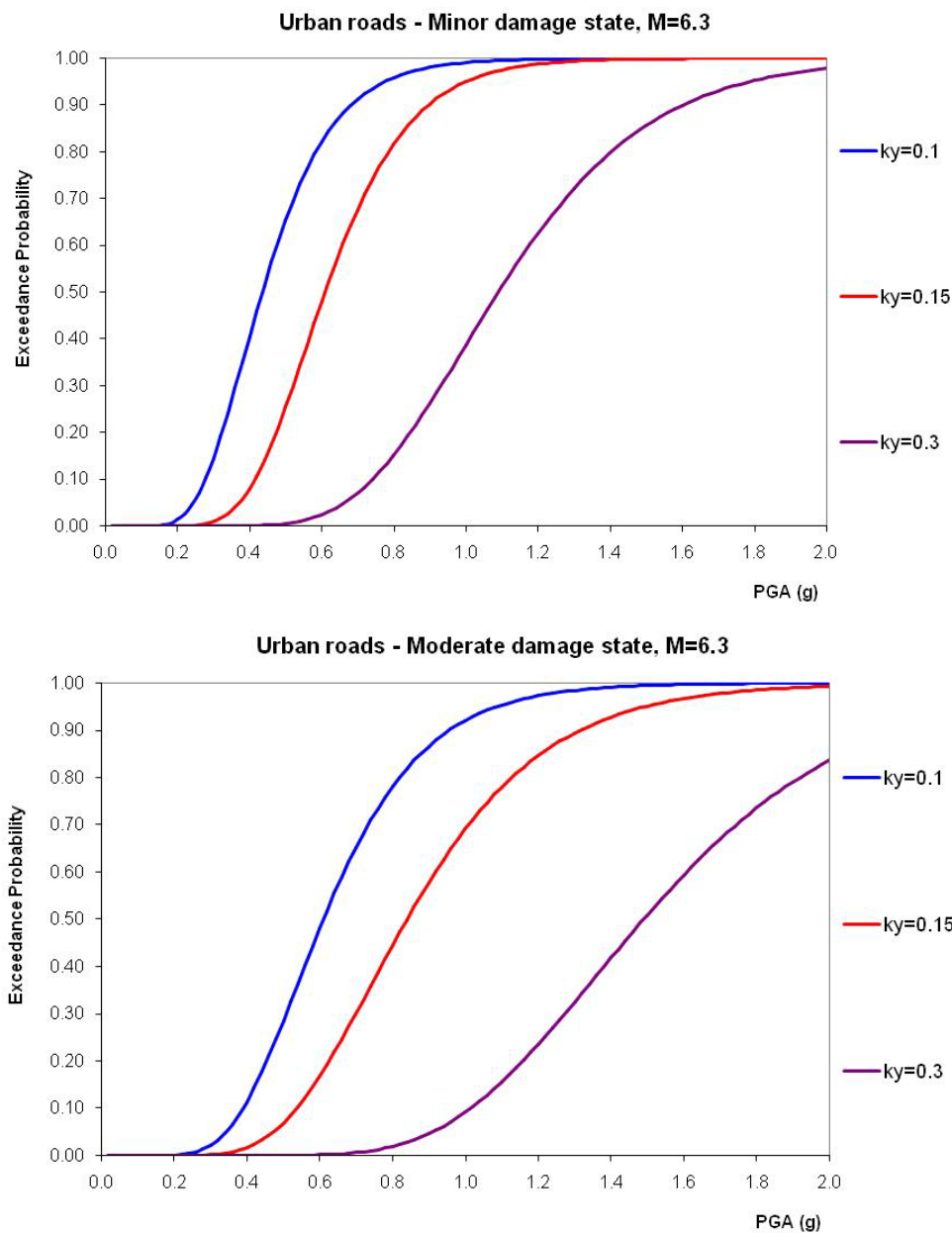| Components		Peak Ground Acceleration					
		k_y=0.1		k_y=0.15		k_y=0.3	
		PGA median (g)	βi	PGA median (g)	βi	PGA median (g)	βi
Urban Road	slight/ minor	0.435	0.35	0.61	0.3	1.09	0.3
	moderate	0.61		0.84	0.35	1.49	
	extensive/complete	0.875	0.4	1.2		2.07	0.35

Figure 6.2.2 Fragility curves at various damage states and different yield coefficients (ky) for urban roads on slope for M=6.3.

Deliverable D2.7   Rev. No: 1
Case studies of environmental and societal impact of landslides –
 Part A: Case studies for environmental (physical) vulnerability   Date: 2011-04-01

Table 6.2.2 provides the percentage of the roads of the network that is expected to sustain damage (worst probable damage state/ i.e. exceeding probability >50%) for each damage state and scenario, while the spatial distribution of the above damages is illustrated in Figures 6.2.3-6.2.5.

Table 6.2.2 *Percentage % of the roads of the network that is expected to sustain damages for each damage state and scenario.*

		Seismic Scenario		
		100 Years	**500 Years**	**1000 Years**
Percentage %	**Slight Damage**	0.00	2.26	10.13
	Moderate Damage	0.00	0.00	0.81
	Extensive/ Complete Damage	0.00	0.00	0.00

According to the results of the above application, the roadway system of Grevena is expected to sustain no damages for the 100 years scenario. For the 500 years scenario, 2.26% of the network is expected to sustain slight damages, while for the 1000 years scenario, 10.13% of the network is expected to sustain slight damages and 0.81% moderate damages. As it was expected the damages are observed in the steep slope regions of the city. For the 1000 years scenario the rate of damages is increased and more road segments expected to suffer important damages. It is worth noting that the level of damage estimated using the aforementioned methodology is less severe compared to the corresponding level of damage anticipated using the HAZUS methodology (Pitilakis et al., 2009).

Deliverable D2.7
Case studies of environmental and societal impact of landslides –
 Part A: Case studies for environmental (physical) vulnerability
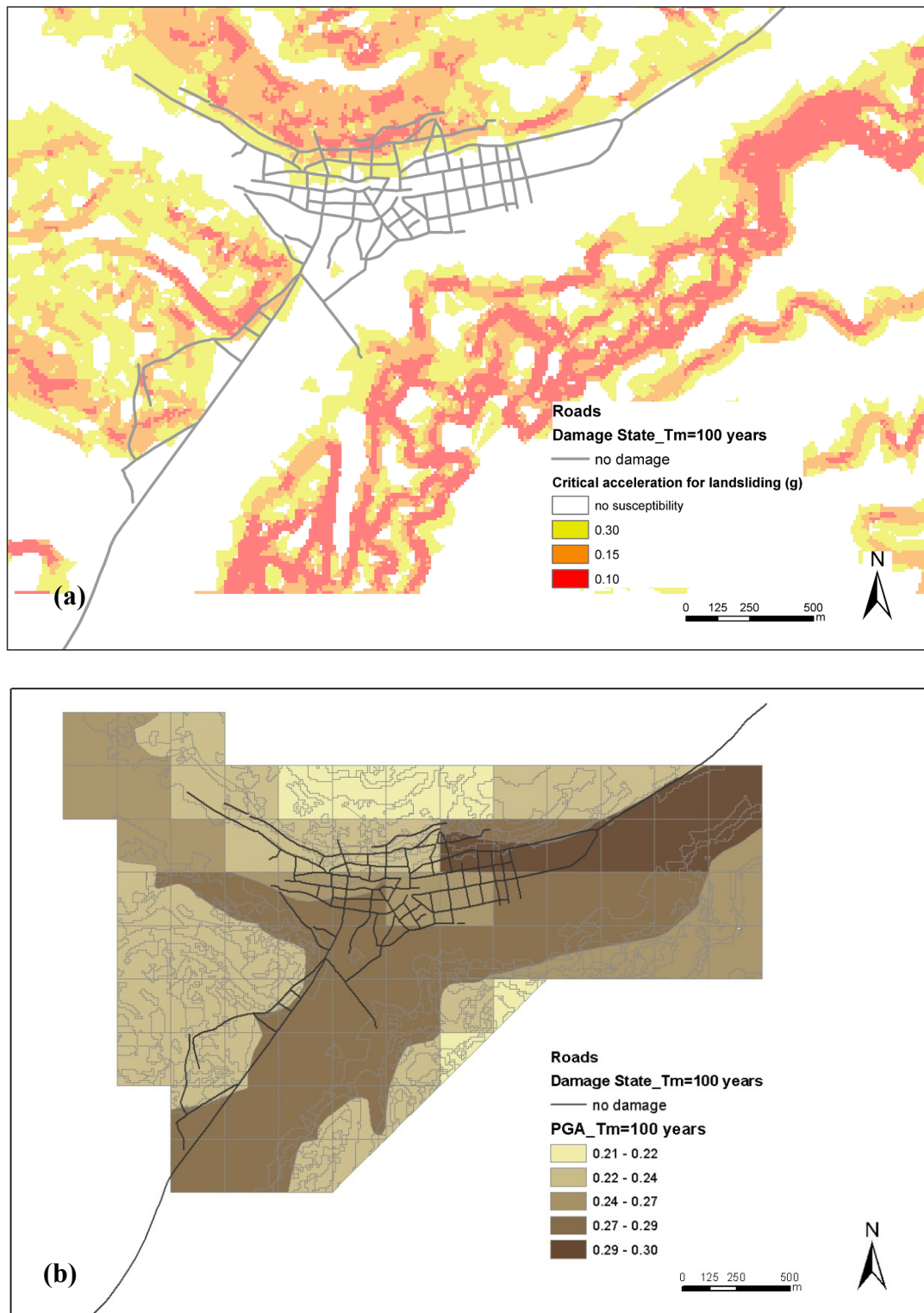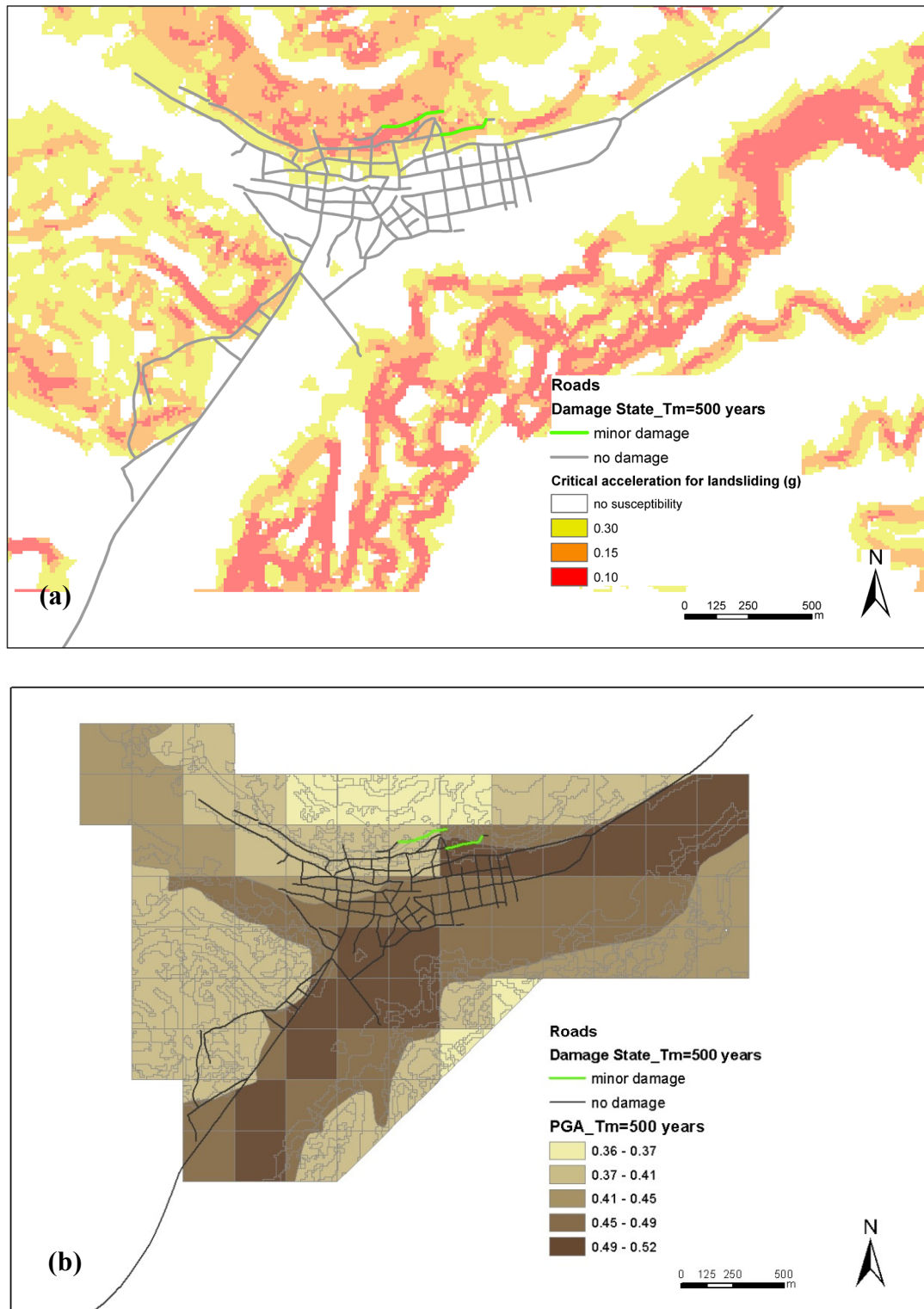
Rev. No: 1

Date: 2011-04-01

Figure 6.2.3 Vulnerability assessment of the roadway system of Grevena due to landsliding for the 100 years seismic scenario. The spatial distribution of critical acceleration (a) and PGA (b) values is also shown.

Deliverable D2.7
Case studies of environmental and societal impact of landslides –
 Part A: Case studies for environmental (physical) vulnerability

Rev. No: 1

Date: 2011-04-01

Figure 6.2.4 Vulnerability assessment of the roadway system of Grevena due to landsliding for the 500 years seismic scenario. The spatial distribution of critical acceleration (a) and PGA (b) values is also shown.

Deliverable D2.7
Case studies of environmental and societal impact of landslides –
Part A: Case studies for environmental (physical) vulnerability
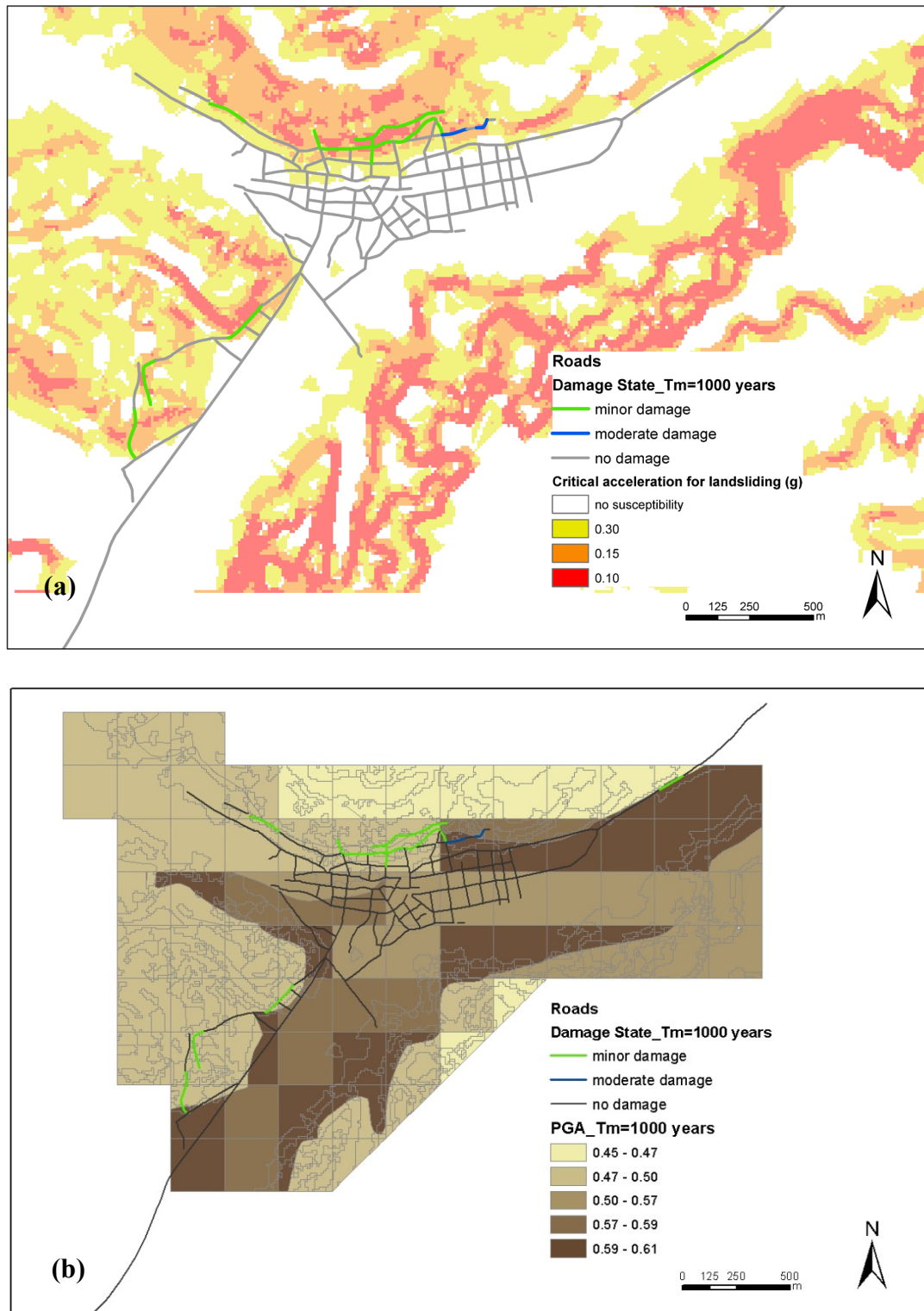
Rev. No: 1

Date: 2011-04-01

Figure 6.2.5 Vulnerability assessment of the roadway system of Grevena due to landsliding for the 1000 years seismic scenario. The spatial distribution of critical acceleration (a) and PGA (b) values is also shown.

Deliverable D2.7   Rev. No: 1
Case studies of environmental and societal impact of landslides –
 Part A: Case studies for environmental (physical) vulnerability   Date: 2011-04-01

7   REFERENCES

Bird, J.F., Crowley, H., Pinho, R. and Bommer, J.J. (2005). "Assessment of building response to liquefaction induced differential ground deformation". Bulletin of the New Zealand Society for Earthquake Engineering, Vol. 38, No. 4, pp. 215-234.

Bray, J.D. and Travasarou, F., (2007). "Simplified Procedure for Estimating Earthquake-Induced Deviatoric Slope Displacements". Journal of Geotechnical and Geoenvironmental Engineering, Vol. 133, No. 4, pp. 381-392.

BRGM (French Geological Survey) Software (1998) Cyberquake, version 1.1. User's guide.

Burland, J.B. (1995): Assessment of risk of damage to buildings due to tunnelling and excavations. Invited special lecture. Proc. 1st International Conference on Earthquake Geotechnical Engineering. IS-Tokyo '95, pp. 1189-1201.

Cascini, L. (1983): Dati preliminari sulla frana di S. Pietro in Guarano. Rapporto Interno del Dipartimento di Difesa del Suolo, Università della Calabria (in Italian).

Cascini, L. (2002): Il rischio da frana in aree urbane dell'Appennino Centro-meridionale. Proceedings of the 21st Italian Geotecnical Congress. L'Aquila, 11-13 September, Vol. 1, pp. 127 – 134, Pàtron Editore, Bologna. ISBN 88-555-2663-4

Cascini, L. (2008): Applicability of landslide susceptibility and hazard zoning at different scales. Engineering Geology, 102, pp. 164-177.

Cascini, L., Critelli, S., Di Nocera, S., Gullà, G. (1992): A methodological approach to landslide hazard assessment: a case history. Proceedings of the 6th International Symposium on Landslides, Christchurch (New Zealand), 10-14 February 1992. Edited by D.H. Bell, Vol. 2, pp. 899-904. A.A. Balkema, Rotterdam.

Cascini, L., Fornaro, G., Peduto, D. (2010): Advanced low- and full-resolution DInSAR map generation for slow-moving landslide analysis at different scales. Engineering Geology, 112 (1-4), 29-42.

Cascini, L., Gullà, G., Sorbino, G. (2006): Groundwater modelling of a weathered gneissic cover. Canadian Geotechnical Journal,43:1153-1166.

Cascini, L., Versace, P. (1988): *Relationship between rainfall and landslide in a gneissic cover.* Proceedings of the 5th International Symposium on Landslides, Lausanne, Swirtzerland. 10-15 July 1988. Edited by Ch. Bonnard. A.A. Balkema, Rotterdam, The Netherlands, Vol. I, pp . 565-570.

Coe, J.A., Godt, J.W., Tachker, P. (2004): Map showing recent (1997-98 El Nino) and historical landslides, Crow Creek and vicinity, Alameda and Contra Costa Counties, California. U.S. Geological Survey Scientific Investigations Map, SIM-2859, 16 p.

Crowley, H., Pinho, R. and Bommer, J.J. (2004). "A probabilistic displacement-based vulnerability assessment procedure for earthquake loss estimation". Bulletin of Earthquake Engineering, Vol. 2, No. 2, pp. 173-219.

Cruden, D.M., Varnes, D.J. (1996): Landslide types and processes. In: Turner, A.T., Schuster, R.L. (Eds.), "Landslides — Investigation and Mitigation", Transportation Research Board Special Report No. 247. National Academy Press, Washington DC, pp. 36–75.

Darendeli, M. (2001). Development of a new family of normalized modulus reduction and material damping curves, *Ph.D. Dissertation*, Univ. of Texas.

Dietrich, W.E., Dunne, T., Humprey, N.S., Reid, L.M. (1982): Construction of sediment budgets far drainage basins. In: Sediment budgets and routing in forested drainage basins. Edited by Swanson F.S., Jande R.J., Dunne T., Swanson D.N.). General Technical Report PNW-141, USDA Forest Service, Pacific Northwest Forest and Range Experiment Station, Portland, Oreg., pp. 5-23.

Ferlisi, S., Pisciotta, G. (2007): A preliminary study of landslide induced property damages towards consequence analysis. Proceedings of the First North American Landslide Conference. Vail

Deliverable D2.7
Case studies of environmental and societal impact of landslides –
 Part A: Case studies for environmental (physical) vulnerability

Rev. No: 1

Date: 2011-04-01

(Colorado), 3-9 June. Editors: V.R. Schuster, R.L. Schuster, A.K. Turner. AEG Publication n. 23. ISBN 978-0-975-4295-3-2. (on CD-ROM).

Fotopoulou, S., Pitilakis, K., (2011). "An analytical approach for the vulnerability assessment of RC buildings subjected to earthquake induced ground displacements", 3rd International Conference on Computational Methods in Structural Dynamics and Earthquake Engineering, M. Papadrakakis, M. Fragiadakis, V. Plevris (eds.) Corfu, Greece, 26–28 May.

Fotopoulou, S., Pitilakis, K., Anagnostopoulos, C. (2011), Vulnerability Assessment of RC buildings due to earthquake induced slow moving slides. 5th International Conference on Earthquake Geotechnical Engineering, Santiago, Chile.

Galli, M., Guzzetti, F. (2007): Landslide Vulnerability Criteria: A Case Study from Umbria, Central Italy. Environ Manage, 40:6, 49–664.

GEO-SLOPE (2004): Stress and deformation modelling with SIGMA/W, user's guide version 6.02. GEO-SLOPE International Ltd., Calgary, Alberta, Canada.

Itasca Consulting Group, Inc. FLAC (Fast Lagrangian Analysis of Continua), ver. 5.0. Itasca Consulting Group, Inc., Minneapolis, 2005.

Mander, J.B., Priestley, M.J.N., Park, R. (1988). "Theoretical stress-strain model for confined concrete", Journal of Structural Engineering, Vol. 114, No. 8, pp. 1804-1826.

Margaris, B. ,G. Athanasopoulos, G. Mylonakis, C. Papaioannou, N. Klimis, N. Theodoulidis, A. Savvaidis, V. Efthymiadou, and J. P. Stewart, (2010). «Mw=6.4 Achaia-Elia (Greece) earthquake on 8 June 2008: Source Characteristics, Ground Motions, and Ground failure», Earthquake Spectra, vol. 26, No 2, pp. 399- 424.

Margaris, B., C. Papaioannou, N. Theodoulidis, A. Savvaidis, N. Klimis, K. Makra, C. Karakostas, V. Lekidis, T. Makarios, T. Salonikios, M. Demosthenus, G. Athanasopoulos, G. Mylonakis, C. Papantonopoulos, V. Efthymiadou, P. Kloukinas, I. Ordonez, V. Vlachakis, and J. P. Stewart (2008). Preliminary report on the principal seismological and engineering aspects of the Mw _ 6:5 Achaia-Ilia (Greece) earthquake on 8 June 2008, GEER Association Report No. GEER-013, http://research.eerc.berkeley.edu/projects/GEER/ Post_EQ_Reports.html (last accessed October 2008).

National Institute of Building Sciences (NIBS) (2004), *Earthquake Loss Estimation Methodology HAZUS 2004, Technical Manual*, FEMA, Washington DC.

Pisciotta, G. (2008): Physical vulnerability of elements at risk in landslide prone areas. PhD Thesis, University of Salerno, Italy.

Pitilakis et al. (2009). "SRM-DGC (Development and proposition for implementation of an efficient methodology and appropriate local instruments for the management, prevention and reduction of seismic risk in Düzce -Turkey, Grevena - Greece and Catania – Italy) Final Report, Part A (2009)", *Final report for the city of Grevena (WP: 1-5)*, Laboratory of Soil Mechanics, Foundations & Geotechnical Earthquake Engineering, Department of Civil Engineering, Aristotle University of Thessaloniki.

Pitilakis K. et al. (2010):").'Physical vulnerability of elements at risk to landslides: Methodology for evaluation, fragility curves and damage states for buildings and lifelines". Deliverable 2.5 in EU FP7 research project No 226479 SafeLand – living with landslide risk in Europe: Assessment, effects of global change, and risk management strategies.

Pitilakis, K., Anastasiadis A., Kakderi K., Manakou M., Manou D., Alexoudi, M., Fotopoulou S., Argyroudis S., Senetakis K., (2011). "Development of comprehensive earthquake loss scenarios for a Greek and a Turkish city: Seismic hazard, Geotechnical and Lifeline Aspects", *Earthquakes and Structures* (accepted for publication).

SeismoSoft (2007). SeismoStruct – A computer program for static and dynamic nonlinear analysis of framed structures, (online): Available from URL: www.seismosoft.com

Skempton A.W., Mac Donald D.H. (1956): Allowable Settlement of Structures. Proc. Institute of Civil Engineers, Part III, Vol. 5, pp. 727-768.

Deliverable D2.7
Case studies of environmental and societal impact of landslides –
 Part A: Case studies for environmental (physical) vulnerability

Rev. No: 1

Date: 2011-04-01

Soeters, R., van Westen, C.J. (1996): Slope instability recognition, analysis and zonation. In A.K. Turner and R.L. Schuster (eds.). Landslides Investigation and Mitigation. TRB Special Report 247, National Academy Press, Washington D.C., 129-177.

Sorbino, G. (1994): Il regime delle acque sotterranee nelle rocce metamorfiche alterate. PhD Thesis, University of Naples "Federico II", Italy.

Viscardi, A. (2010): Gli effetti indotti sul costruito da frane a cinematica lenta. PhD Thesis, University of Salerno, Italy.

Wong, H.N., Ho, K.K.S., Chan, Y.C. (1997): Assessment of consequence of landslides. Proceedings of the International Workshop on Landslide Risk Assessment, Honolulu, Hawaii (USA), A.A. Balkema Publishers, pp. 111-147.